



Exploring heavy nuclei using lifetime measurements of excited states

Christoph Fransen

Institut für Kernphysik, Universität zu Köln, Cologne, Germany

ESNT Workshop Saclay, November 2015

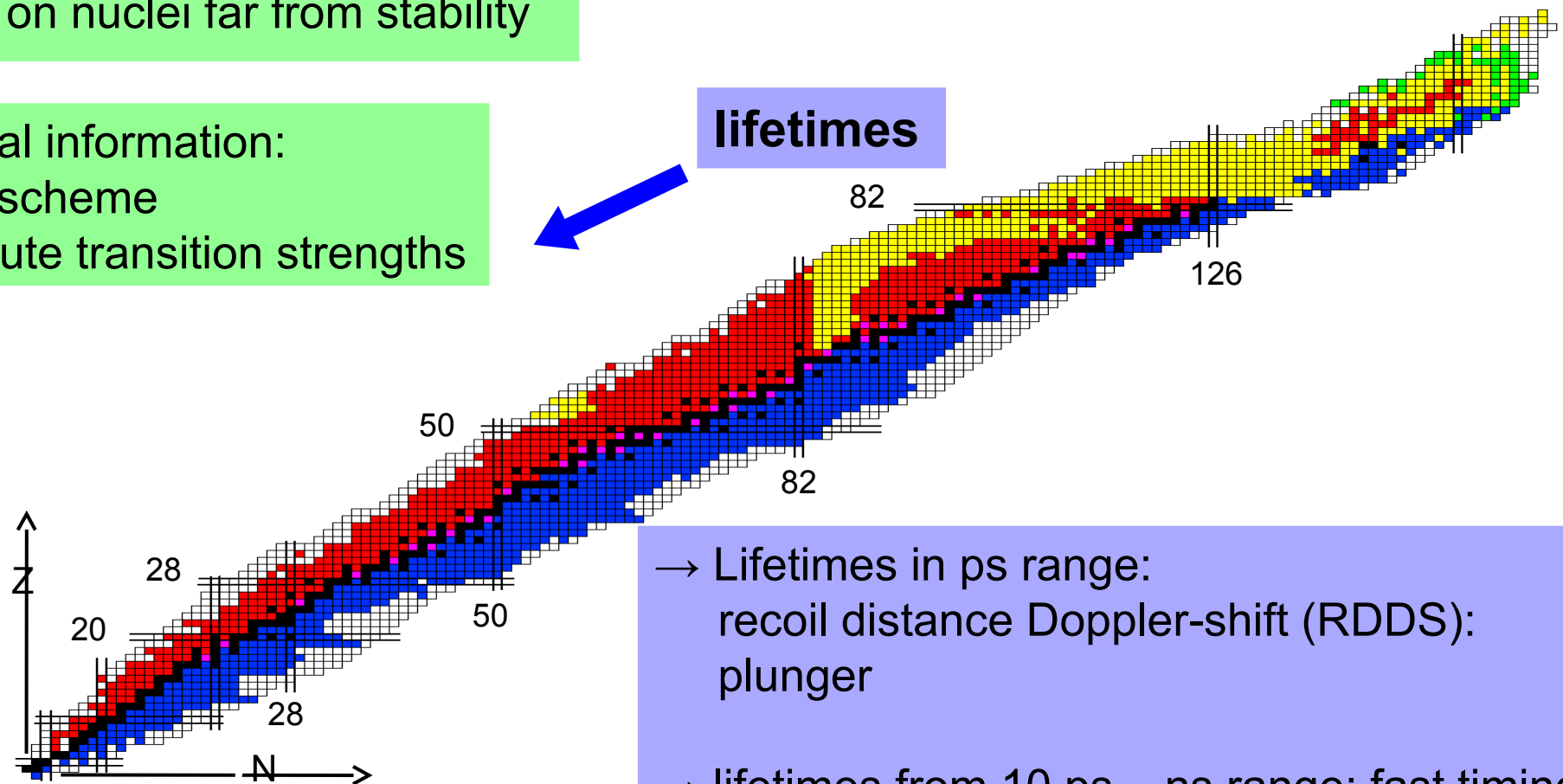
Outline

1. Introduction
2. The plunger technique
3. Other lifetime techniques used by our group:
 - a. Fast timing
 - b. Doppler-shift attenuation method
4. Shape coexistence in neutron deficient Hg isotopes
5. Critical point symmetries in the $A=180$ mass region
6. Search for isovector excitations in the vicinity of ^{208}Pb

Introduction

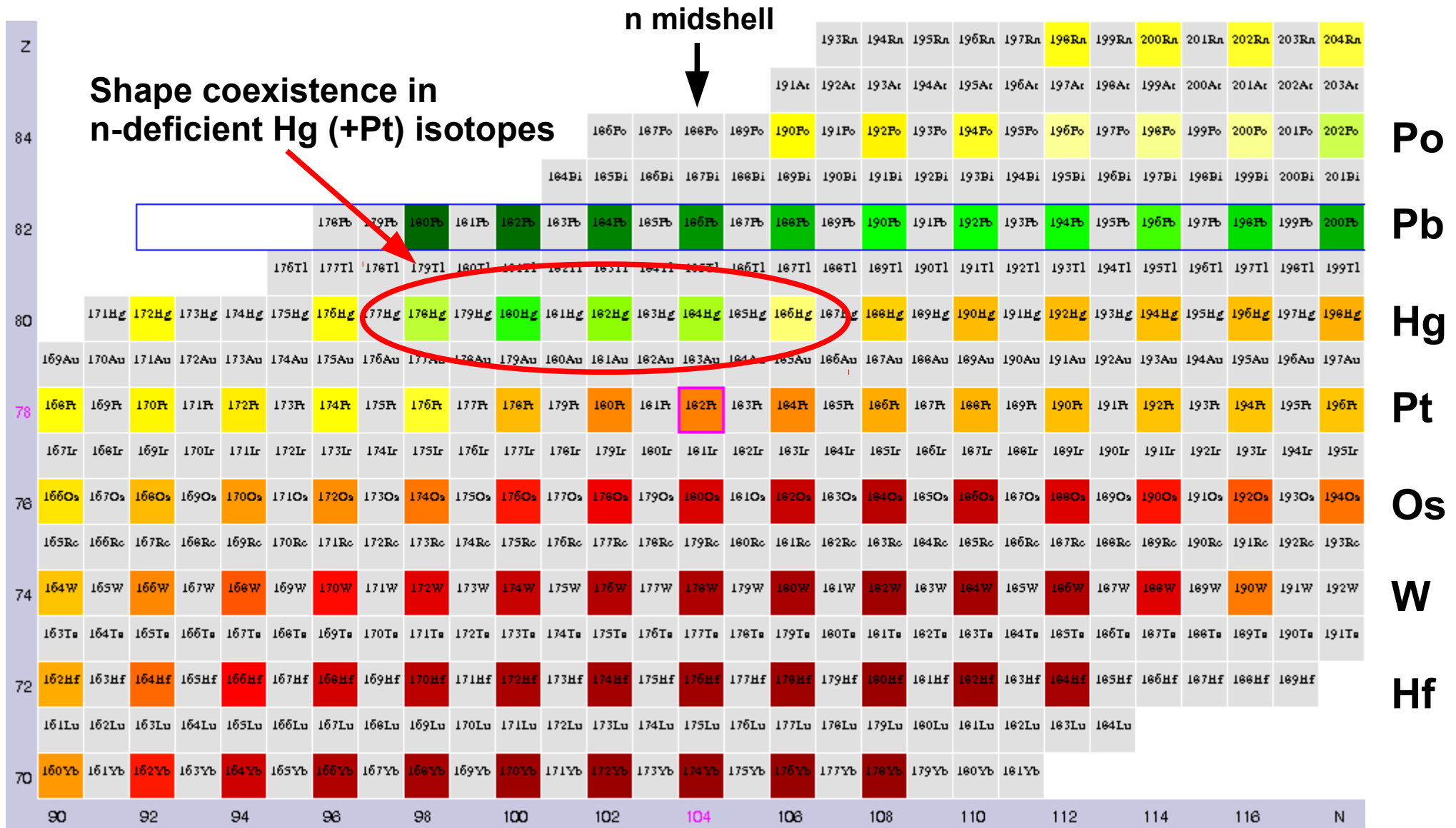
Present nuclear physics:
focus on nuclei far from stability

Crucial information:
level scheme
absolute transition strengths



- Lifetimes in ps range:
recoil distance Doppler-shift (RDDS):
plunger
- lifetimes from 10 ps – ns range: fast timing
- lifetimes in fs range:
Doppler-shift attenuation method (DSAM)

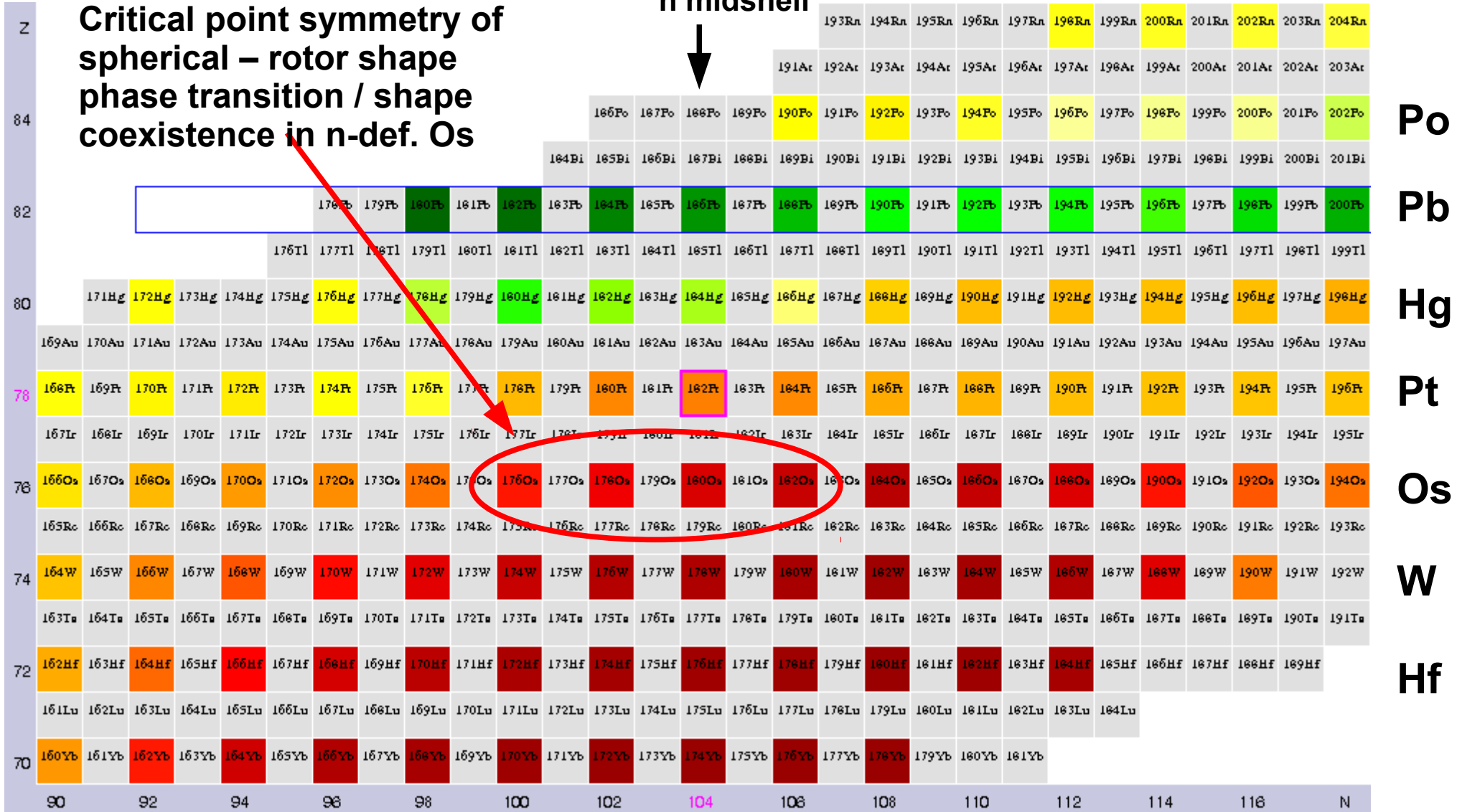
Introduction



Introduction

Critical point symmetry of spherical – rotor shape phase transition / shape coexistence in n-def. Os

n midshell



Introduction

Low-lying isovector 2^+
valence shell excitation in ^{212}Po

N=126



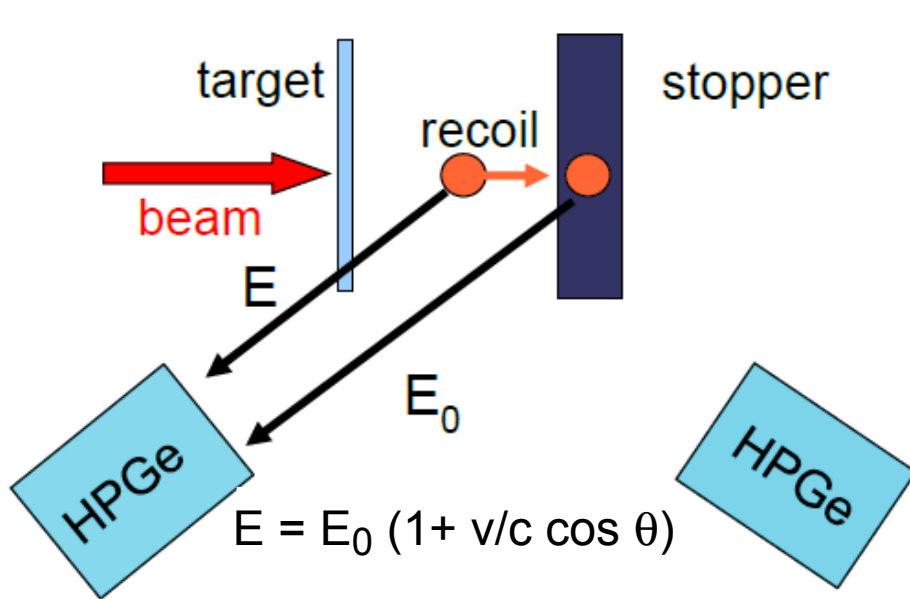
Z=82



Outline

1. Introduction
2. The plunger technique
3. Other lifetime techniques used by our group:
 - a. Fast timing
 - b. Doppler-shift attenuation method
4. Shape coexistence in neutron deficient Hg isotopes
5. Critical point symmetries in the $A=180$ mass region
6. Search for isovector excitations in the vicinity of ^{208}Pb

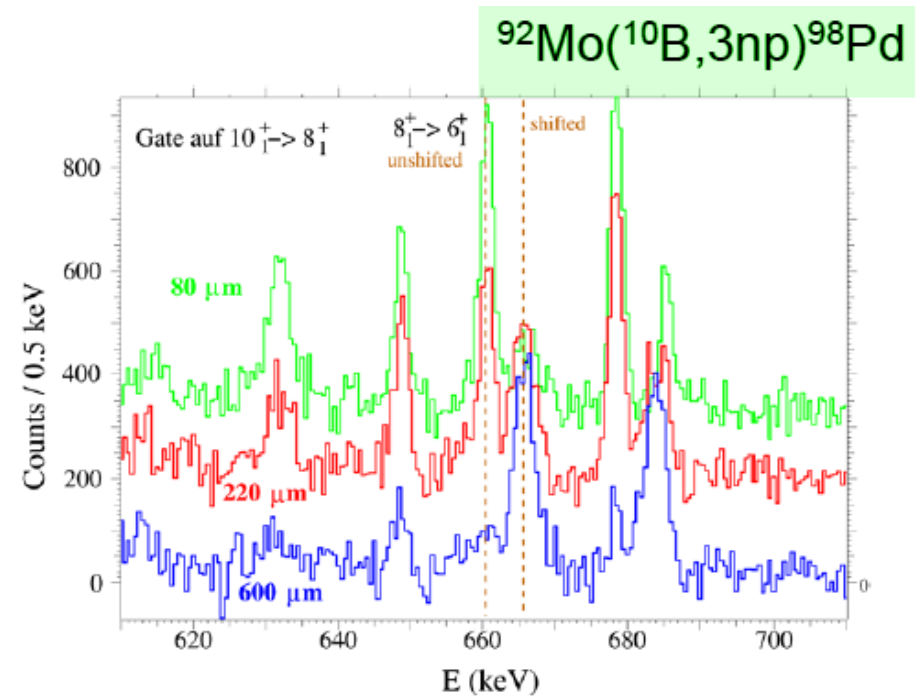
The plunger technique



$$\tau(t_k) = \frac{I^{\text{us}}(t_k)}{\frac{d}{dt} I^{\text{sh}}(t_k)}$$

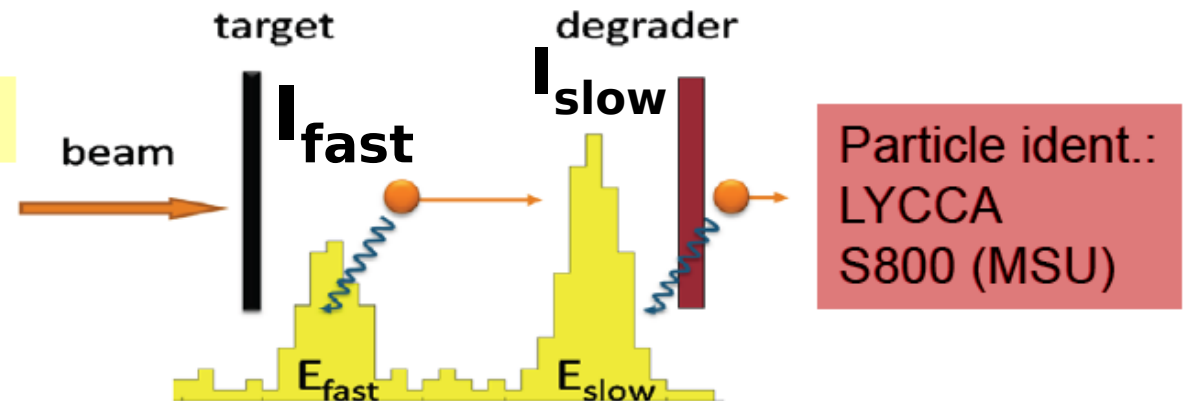
I^{us} = Intensity of the unshifted γ -ray line

I^{sh} = Intensity of the Doppler-shifted component



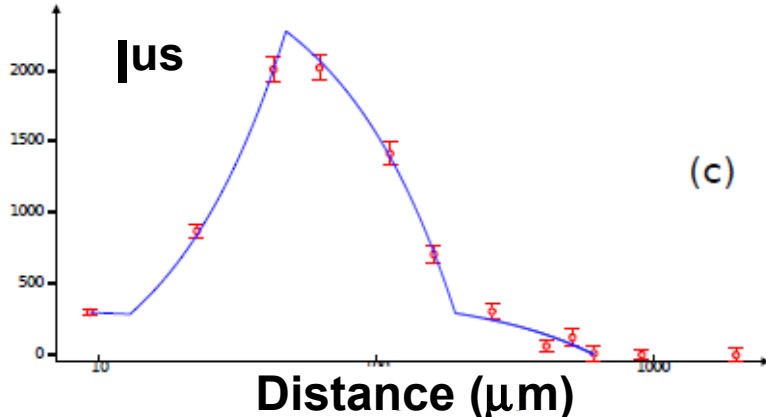
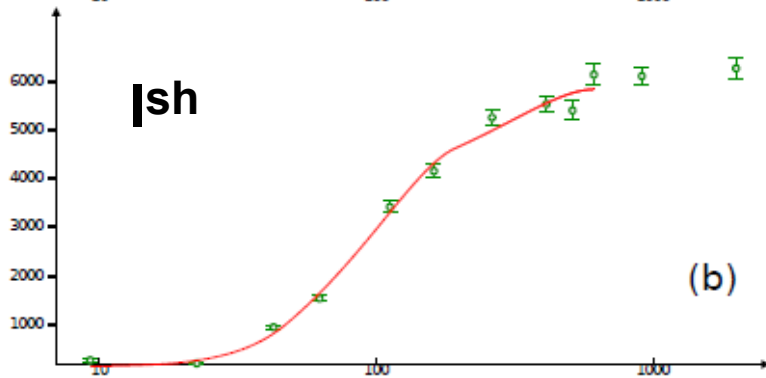
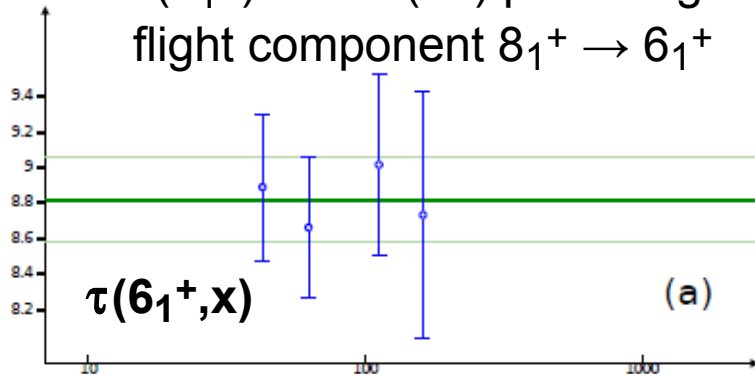
Differential Plunger

Use degrader instead of stopper to allow identification of recoils



The plunger technique

$\gamma\gamma$ coincidence exp. on ^{184}Hg :
 $\tau(6_1^+) = 8.82(24)$ ps from gate on
 flight component $8_1^+ \rightarrow 6_1^+$



Plot ratio $I^{us} / (I^{us} + I^{sh})$ versus target – stopper distance

Every distance in sensitive range gives a lifetime value.

**Differential Decay Curve Method (DDCM)
 Allows to easily discover systematic errors**

$$\tau(t_k) = \frac{I^{us}(t_k)}{\frac{d}{dt} I^{sh}(t_k)}$$

I^{us} = Intensity of the unshifted γ -ray line

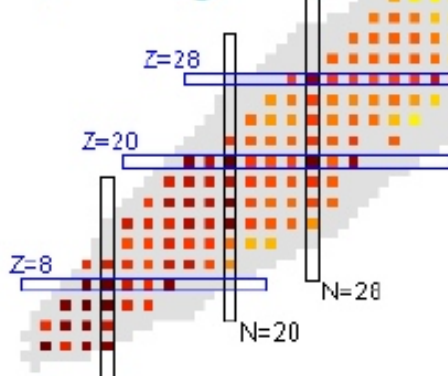
I^{sh} = Intensity of the Doppler-shifted component

Different plunger devices...

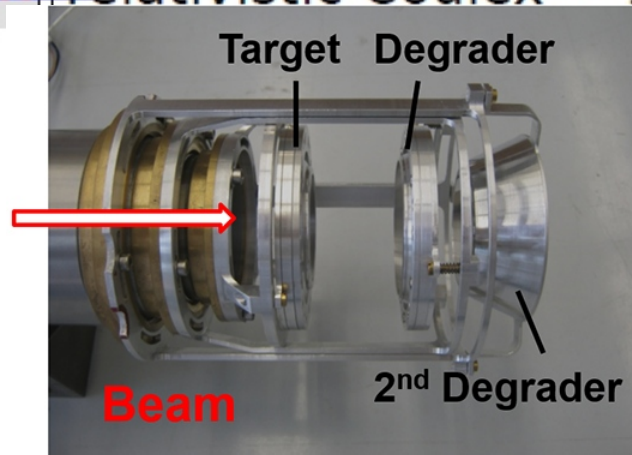
relativistic Coulex
 ~ 200 MeV/u



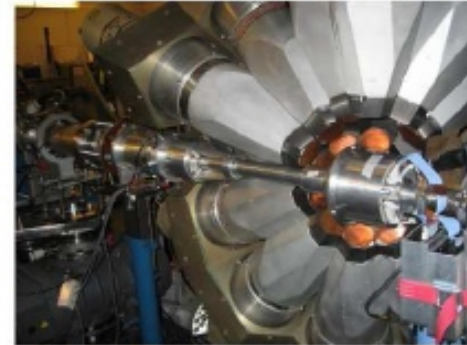
(54 Cr @ GSI)



Knock-out and relativistic Coulex ~ 100 MeV/u

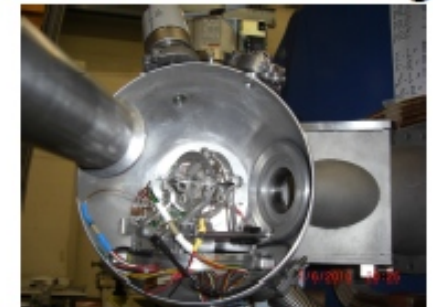


Fusion-evaporation
 Safe Coulex inverse kinematics



178Pt @ iThemba
 180Pt @ JYFL
 178Hg @ JYFL
 184,186,188Hg @ ANL
 n-def. Os @ Cologne
 ... and several more

Deep-inelastic scattering

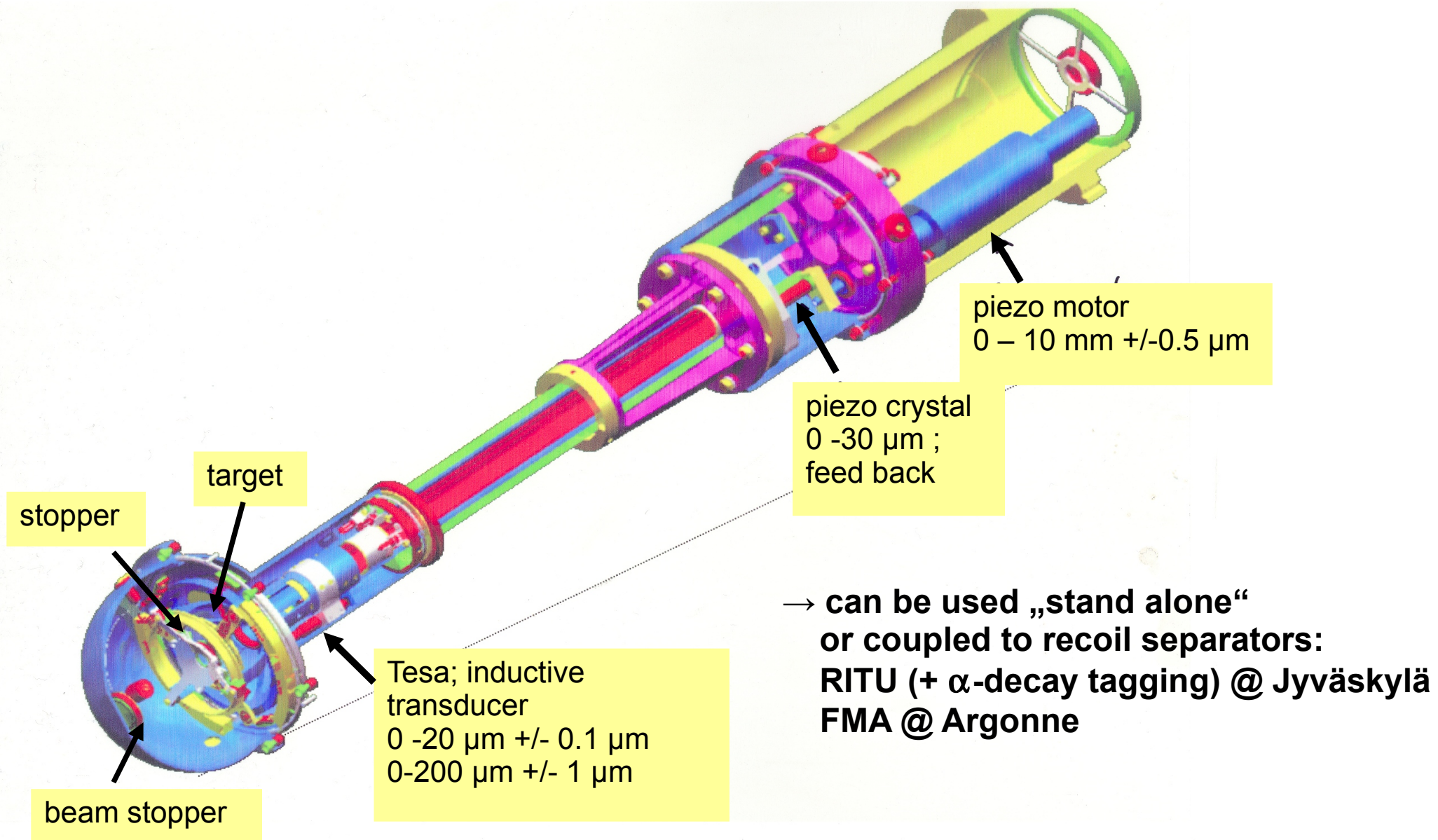


58,60,62 Cr
 @ NSCL

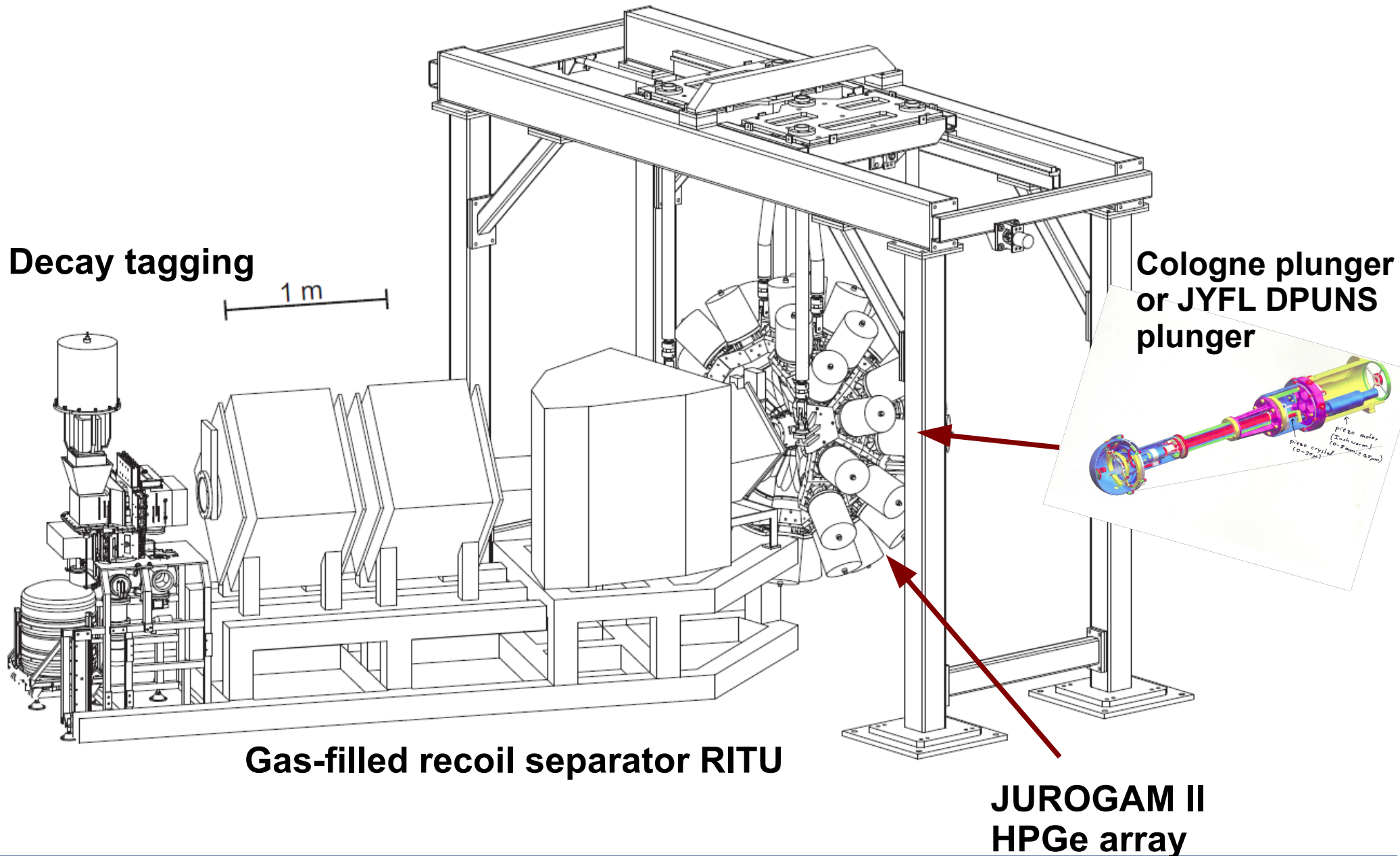
63, 65Co, 62,64 Fe @ GANIL
 A=200 mass region @ GANIL

TRIPLEX plunger
 H. Iwasaki, NSCL

The Cologne „standard“ plunger: Fusion-evaporation, low-energy coulex, ...



The plunger at the recoil separator RITU



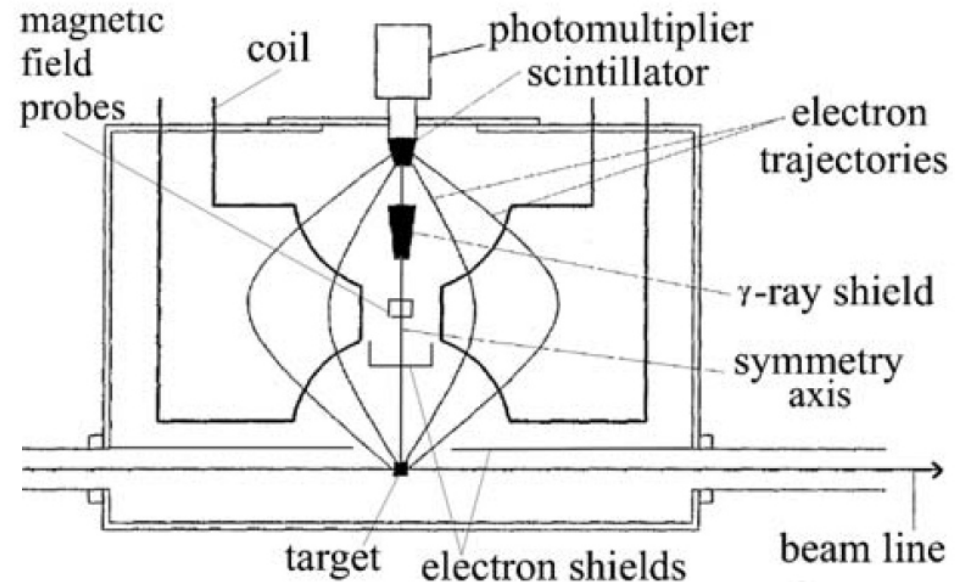
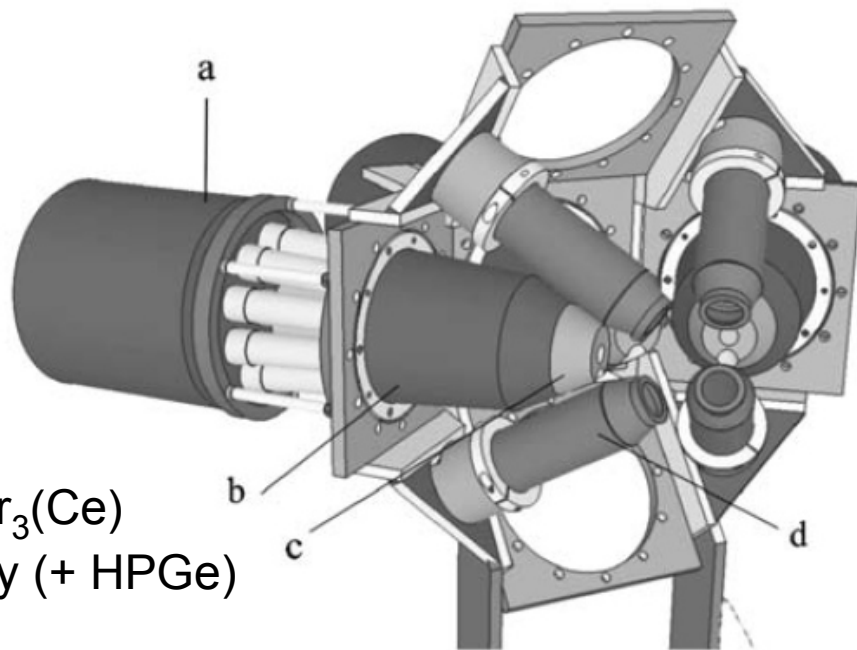
Outline

1. Introduction
2. The plunger technique
3. Other lifetime techniques used by our group:
 - a. Fast timing
 - b. Doppler-shift attenuation method
4. Shape coexistence in neutron deficient Hg isotopes
5. Critical point symmetries in the $A=180$ mass region
6. Search for isovector excitations in the vicinity of ^{208}Pb

Fast timing

- level lifetimes from delayed coincidences between populating and depopulating transitions.
- fast detectors: $\gamma - \gamma$ coincidences between $\text{LaBr}_3(\text{Ce})$ detectors: FWHM = 200 ps or conversion electron (ce) – γ coincidences for transitions with large conversion factors.
- lifetime range: ~ns – 10 ps

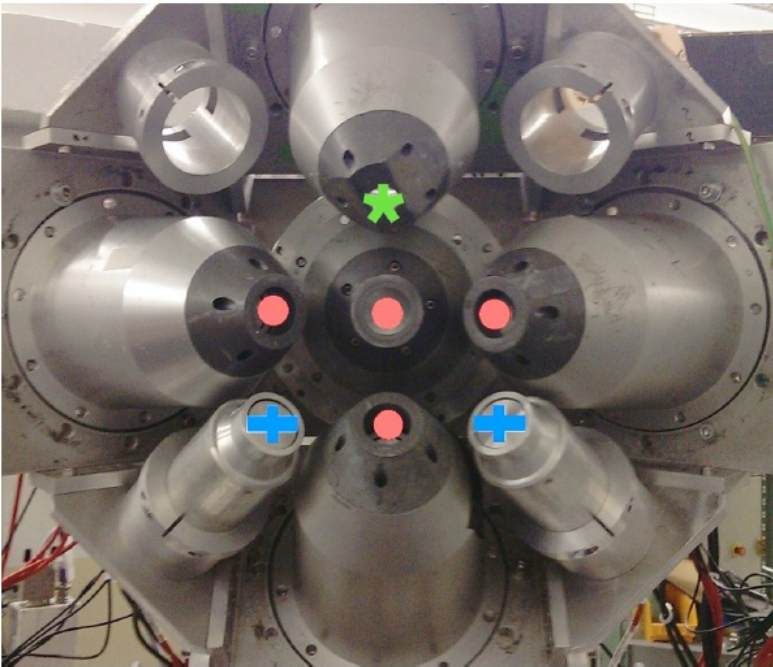
Orange e- spectrometer



Setup at IKP Cologne for fast timing measurements using ce – γ coincidences

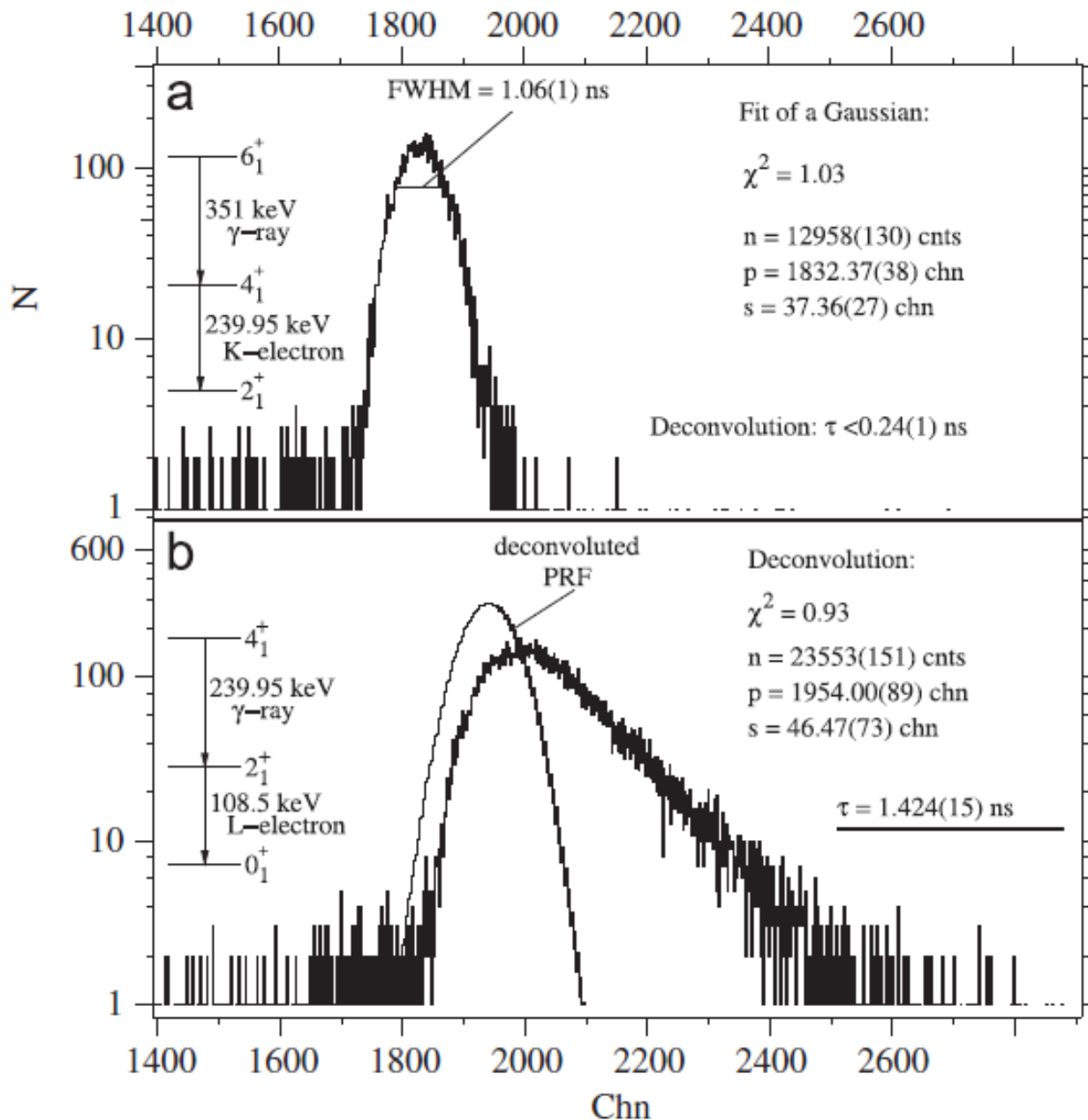
Fast timing

- level lifetimes from delayed coincidences between populating and depopulating transitions.
- fast detectors: $\gamma - \gamma$ coincidences between $\text{LaBr}_3(\text{Ce})$ detectors: FWHM = 200 ps or conversion electron (ce) – γ coincidences for transitions with large conversion factors.
- lifetime range: ~ns – 10 ps



Setup at IKP Cologne
for fast timing measurements
using $\gamma - \gamma$ coincidences between
 $\text{LaBr}_3(\text{Ce})$ detectors with anti-Compton shields
„●“, and unshielded „+“

Example: $\tau(2_1^+)$ in ^{176}W from $e^- - \gamma$ time distribution

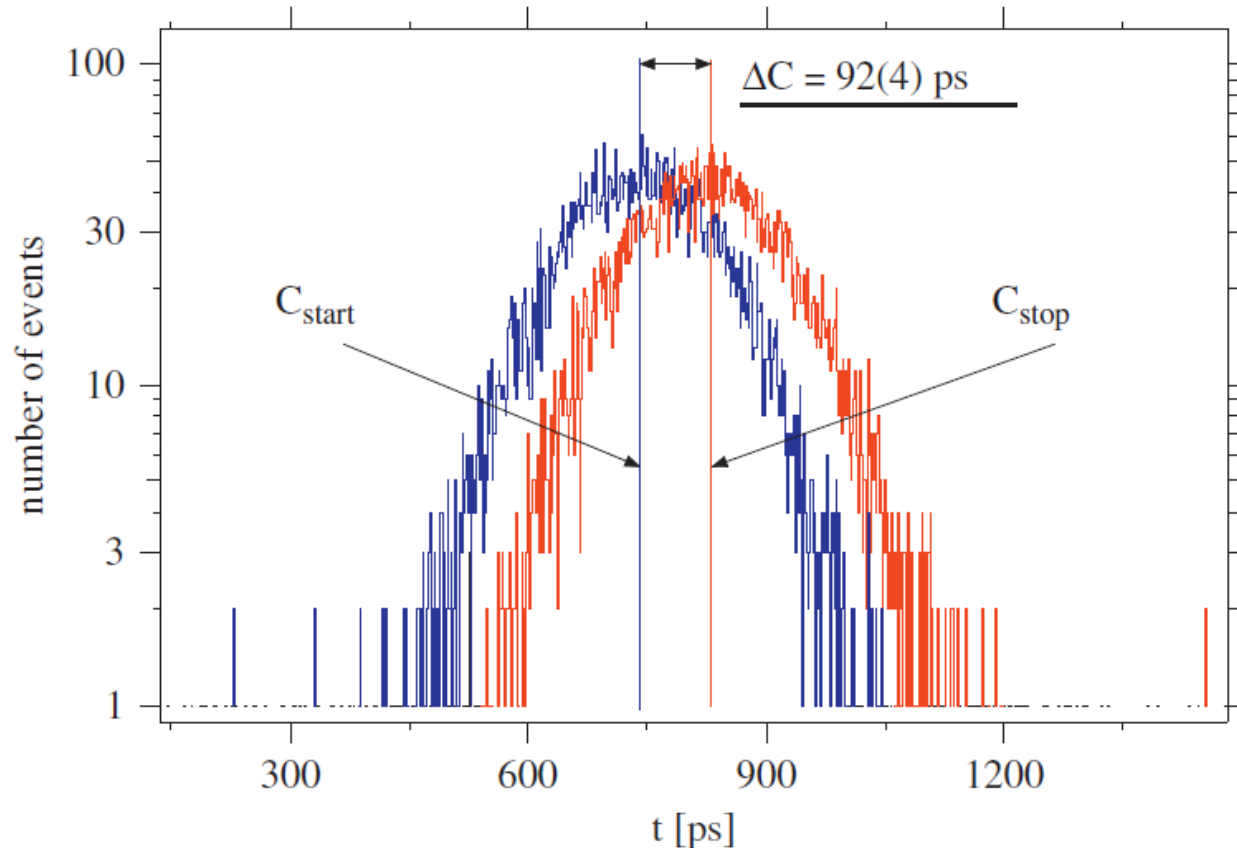


→ deconvolute prompt response function and time response function of level of interest.

→ calibr.: 12.1 ps/chn

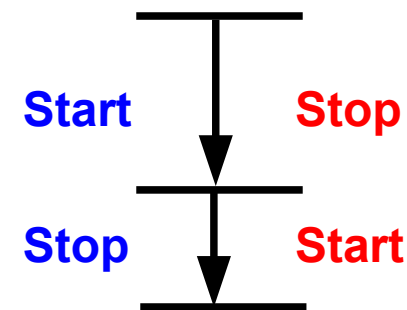
J.M. Regis et al.,
NIM A 606, 466 (09)

Picosecond sensitive fast timing: Mirror symmetric centroid difference method



Two LaBr₃(Ce) detectors:

$$\Delta C(\Delta E_\gamma)_{\text{decay}} = \text{PRD}(\Delta E_\gamma)_{\text{decay}} + 2\tau$$



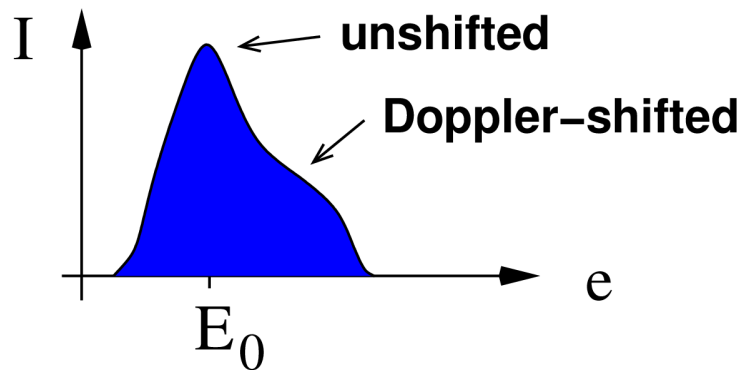
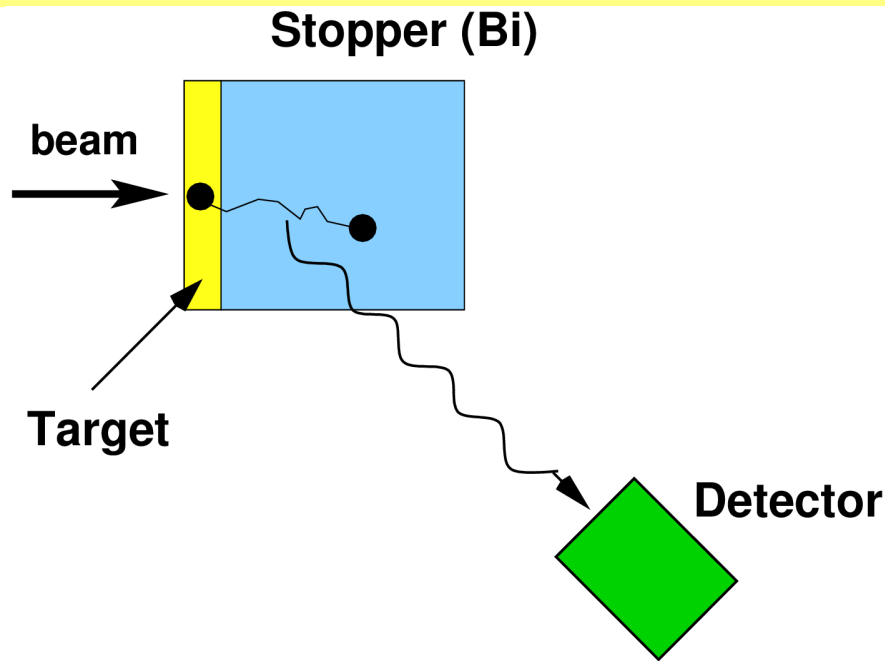
Fast timing array with N equal detectors:
Individual time-walk characteristics treated stochastic:

$$\overline{\Delta C}(E_\gamma) = \overline{\text{PRD}}(E_\gamma) + 2\tau$$

→ Generalized Centroid Difference Method

J.M. Regis et al.,
NIM A 726, 191 (13)

Determination of lifetimes in the sub-ps range: The Doppler-shift attenuation method (DSAM)



$$L'(\tau, v) = \int_0^{\infty} N(v, t) r(t, \tau) dt$$

$$L'(\tau, v) \rightarrow L'(\tau, E)$$

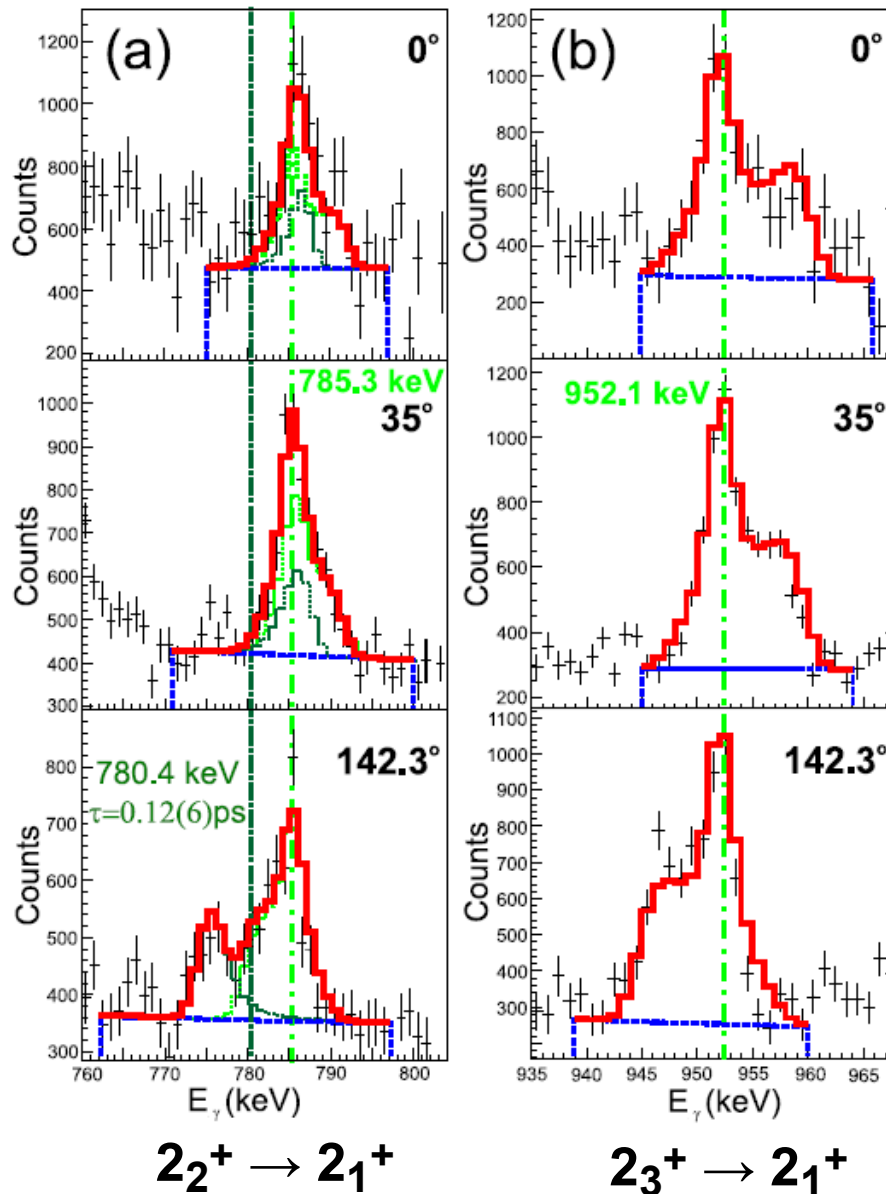
$$L(\tau, E) = \int_{E_{min}}^{E_{max}} L'(\tau, e) f(e, \sigma) de$$

$$f(e, \sigma) = \frac{1}{\sqrt{2\pi}\sigma} \cdot e^{-\frac{(e-E_0)^2}{2\sigma^2}}$$

- Simulate slowing down (Monte Carlo/GEANT4)
- use (semi-empiric) electronic stopping powers and nuclear stopping
- include angular straggling due to nuclear collisions.

P. Petkov: DSAM analysis using DDCM

Determination of lifetimes in the sub-ps range: The Doppler-shift attenuation method (DSAM)



Example:
Determination of lifetimes
of the 2_2^+ and 2_3^+ states
in ^{212}Po

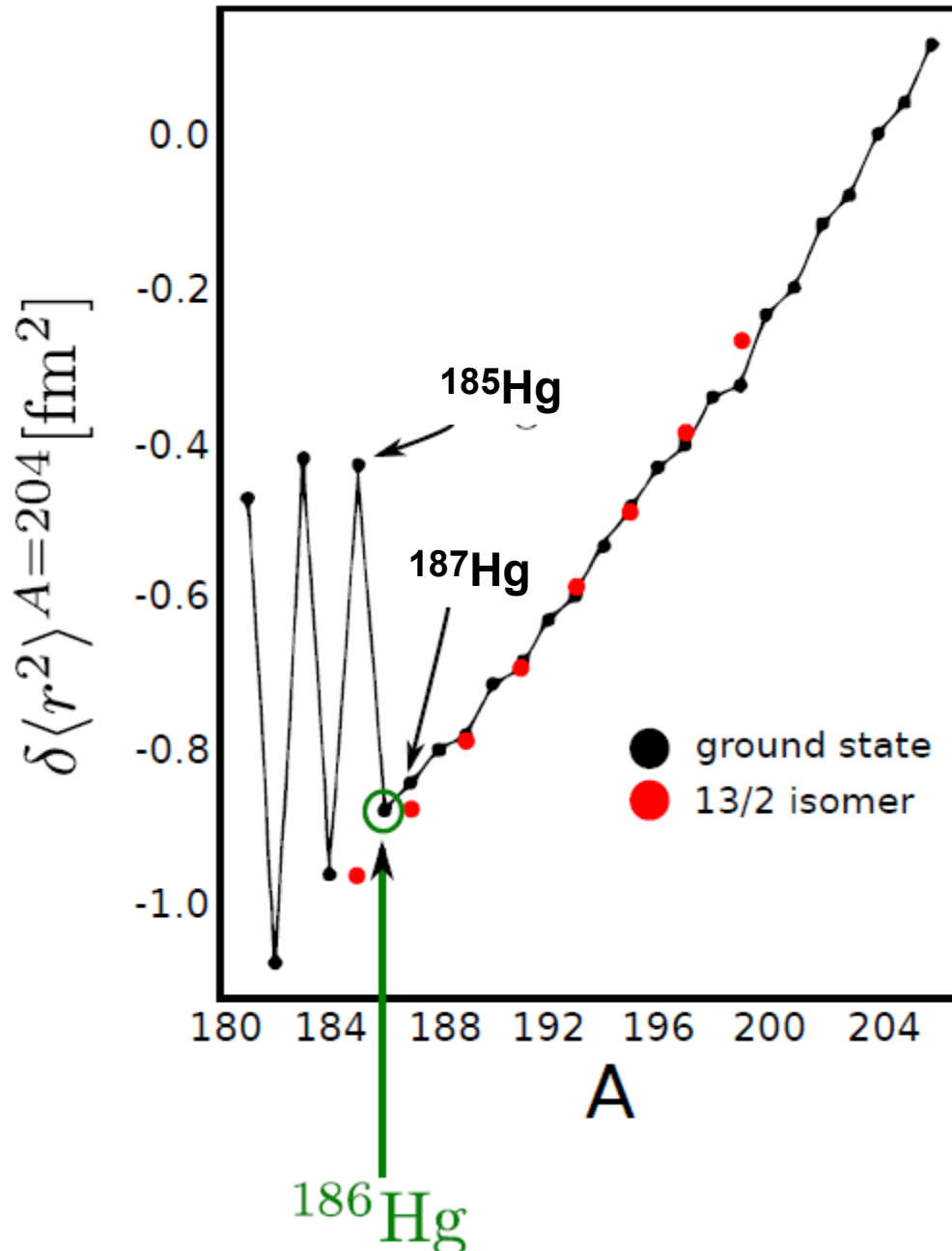
(G. Rainovski, D. Kocheva)
 $^{208}\text{Pb}(^{12}\text{C}, ^8\text{Be})^{212}\text{Po}$
@ Cologne FN Tandem

952.1 keV
 $\tau = 0.80(3)$ ps

Outline

1. Introduction
2. The plunger technique
3. Other lifetime techniques used by our group:
 - a. Fast timing
 - b. Doppler-shift attenuation method
4. Shape coexistence in neutron deficient Hg isotopes
5. Critical point symmetries in the $A=180$ mass region
6. Search for isovector excitations in the vicinity of ^{208}Pb

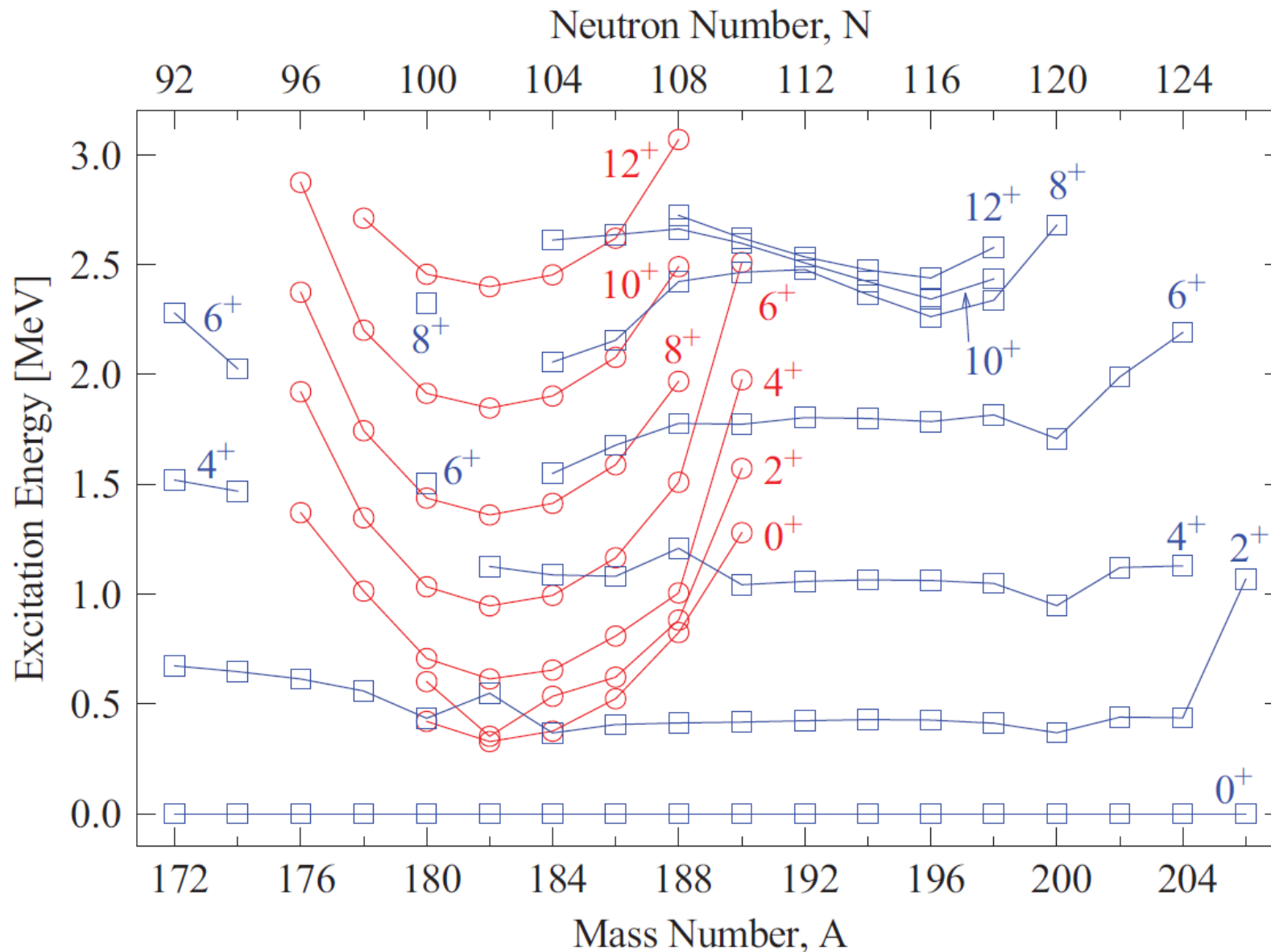
Shape coexistence in light Hg isotopes



S. Frauendorf, S.V. Pashkevich,
PLB 55, 365 (1975):

Sharp change in mean-square radius
 $^{187}\text{Hg} \rightarrow ^{185}\text{Hg}$: evidence for transition
weakly oblate \rightarrow prolate deformed

Shape coexistence in light Hg isotopes: excitation energies



From L. Gaffney et al., PRC 89, 024307 (14)

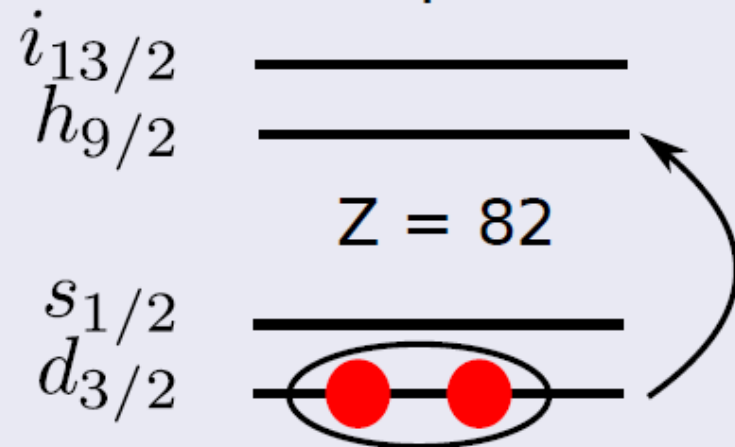
Shape coexistence in light Hg isotopes

Several theoretical approaches

- $\pi(0p - 2h)$ and $\pi(2p - 4h)$, e.g., W. Nazarewicz et al Phys. Lett. B., 305 (1993) 195-201
- J.L. Wood et al Phys. Rep. 215 (1992) 101-201
- IBM, R. Fossion et. al., Phys. Rev. C 67, 024306 (2003)
- Self-consistent Mean Field + particle number restoration: T. Duguet et al, Phys. Lett B 559 (2003) 201; M. Bender et. al., J. Phys. G: Nucl. Part. Phys. 31 (2005) S1611-S1616
- Rel. Mean Field + BCS, e.g. S. Yoshida, Phys. Rev. C 55 (1997) 3, Vretenar et al.

Shell-model picture

Shell-model picture



Second collective excitation:
rotational band on 2p-4h
excitation

Shape coexistence in light Hg isotopes

Several theoretical approaches

- $\pi(0p - 2h)$ and $\pi(2p - 4h)$, e.g., W. Nazarewicz et al Phys. Lett. B., 305 (1993) 195-201
- J.L. Wood et al Phys. Rep. 215 (1992) 101-201
- IBM, R. Fossion et. al., Phys. Rev. C 67, 024306 (2003)
- Self-consistent Mean Field + particle number restoration: T. Duguet et al, Phys. Lett B 559 (2003) 201; M. Bender et. al., J. Phys. G: Nucl. Part. Phys. 31 (2005) S1611-S1616
- Rel. Mean Field + BCS, e.g. S. Yoshida, Phys. Rev. C 55 (1997) 3, Vretenar et al.

Interacting Boson Model

Interacting Boson Model:
low-lying excitations, valence electrons paired to s,d bosons
For ^{186}Pb :

$$\hat{H} = \hat{H}_{reg} + \hat{H}_{2p2h} + \hat{H}_{4p4h} + \hat{V}_{mix}$$

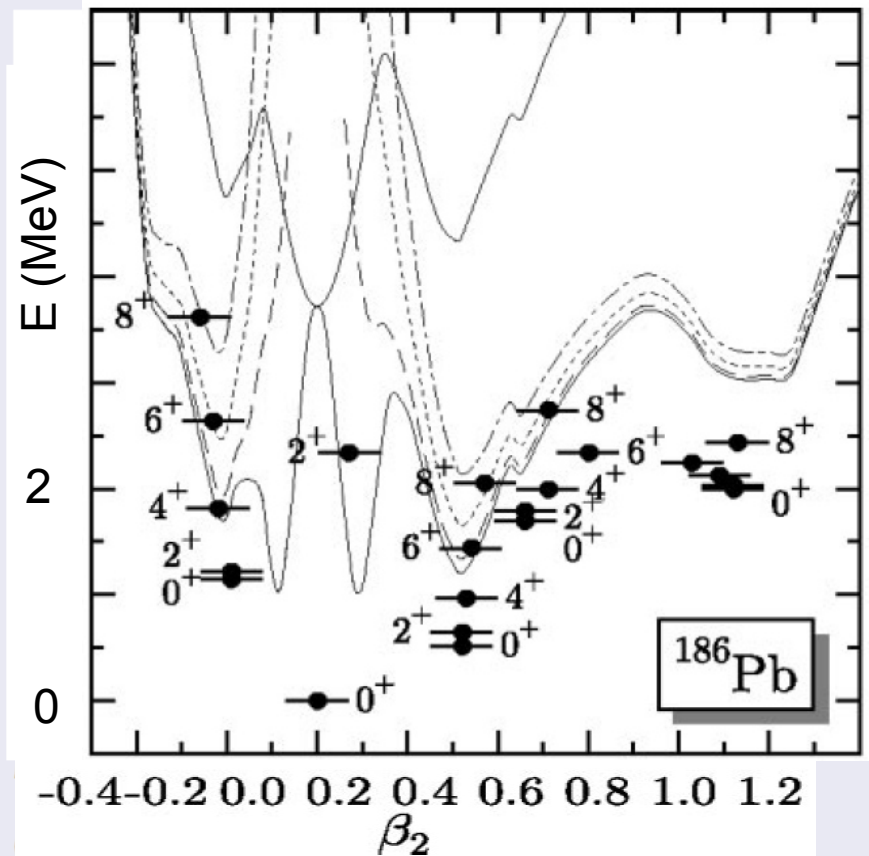
$$\begin{aligned} \hat{H}_{2p2h} &= \epsilon_{2p2h} \hat{n}_d \\ &+ \kappa_{2p2h} \hat{Q}_{2p2h} \cdot \hat{Q}_{2p2h} + \Delta_{2p2h} \end{aligned}$$

Hamiltonians for individual excitations + mixing term

Shape coexistence in light Hg isotopes

Several theoretical approaches

- $\pi(0p - 2h)$ and $\pi(2p - 4h)$, e.g., W. Nazarewicz et al Phys. Lett. B., 305 (1993) 195-201
- J.L. Wood et al Phys. Rep. 215 (1992) 101-201
- IBM, R. Fossion et. al., Phys. Rev. C 67, 024306 (2003)
- Self-consistent Mean Field + particle number restoration: T. Duguet et al, Phys. Lett B 559 (2003) 201; M. Bender et. al., J. Phys. G: Nucl. Part. Phys. 31 (2005) S1611-S1616
- Rel. Mean Field + BCS, e.g. S. Yoshida, Phys. Rev. C 55 (1997) 3, Vretenar et al.

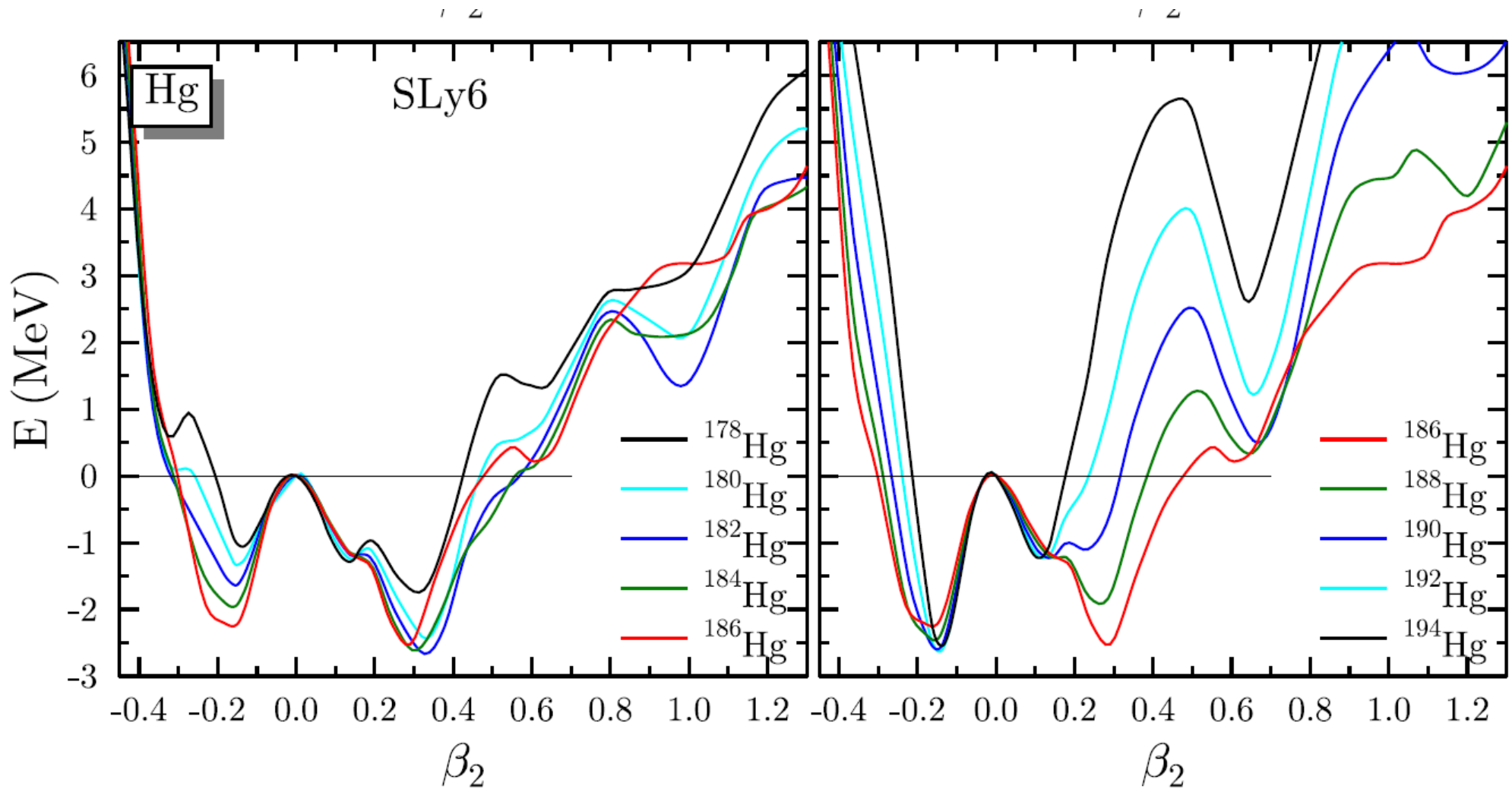


M. Bender et al., PRC 69, 064303 (04)

Configuration mixing of angular momentum and particle projected self-consistent mean field states, Skyrme interaction SLy6

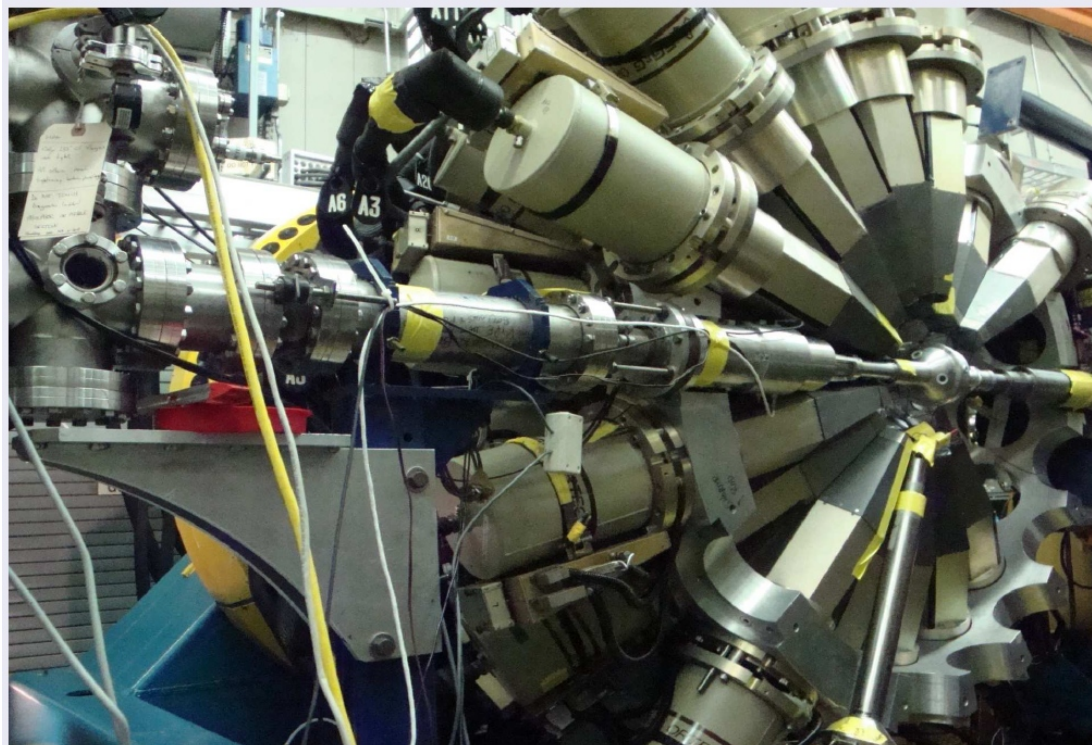
→ shape coex. in Pb isotopes

Systematic microscopic energy density calculations for Hg isotopes (SLy6, M. Bender, Bordeaux)



J.M. Yao, M. Bender, P.-H. Heenen, PRC 87, 034322 (12)

Plunger experiments on $^{184,186}\text{Hg}$ @ ANL

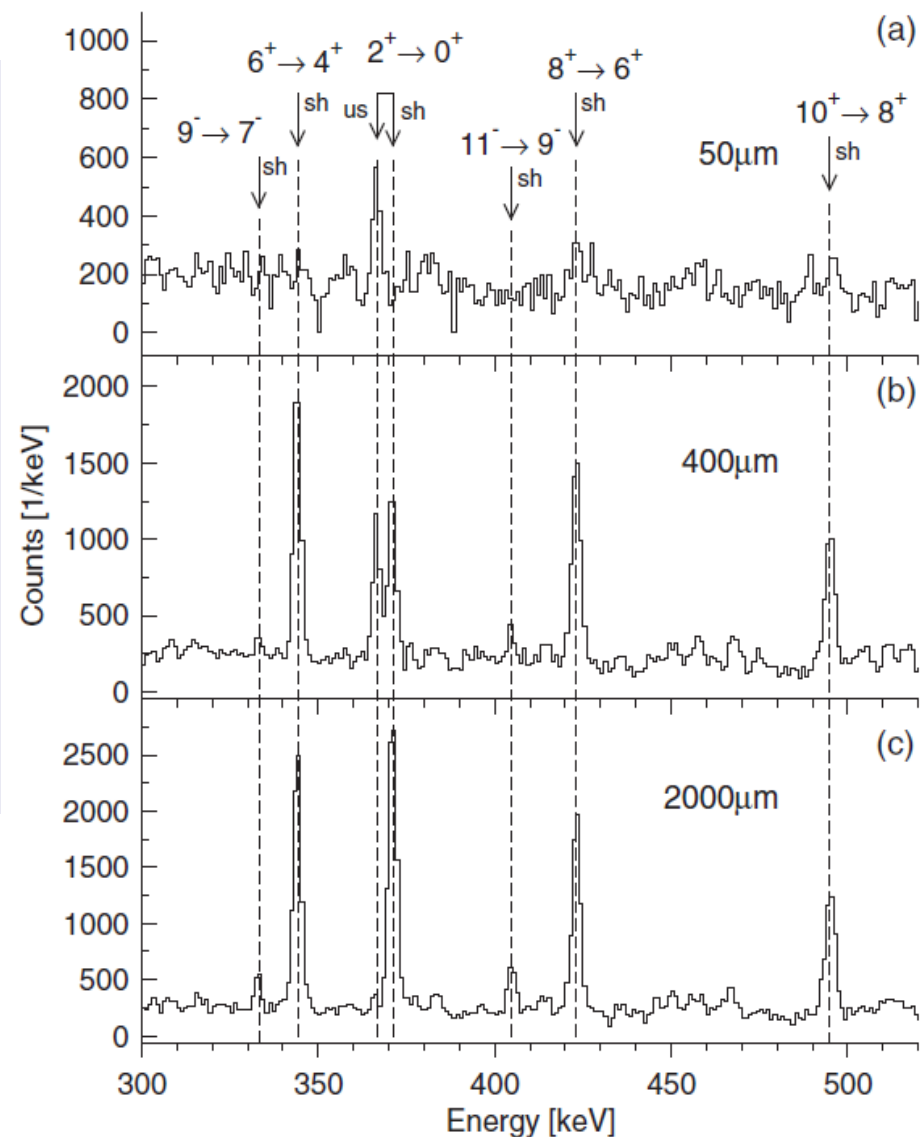


Cologne plunger @ GAMMASPHERE

$^{148}\text{Sm}(^{40}\text{Ar},4n)^{184}\text{Hg}$, $E(^{40}\text{Ar}) = 200 \text{ MeV}$

$^{150}\text{Sm}(^{40}\text{Ar},4n)^{186}\text{Hg}$, $E(^{40}\text{Ar}) = 195 \text{ MeV}$

L. Gaffney, M. Hackstein et al.,
Phys. Rev. C 89, 024307 (14)

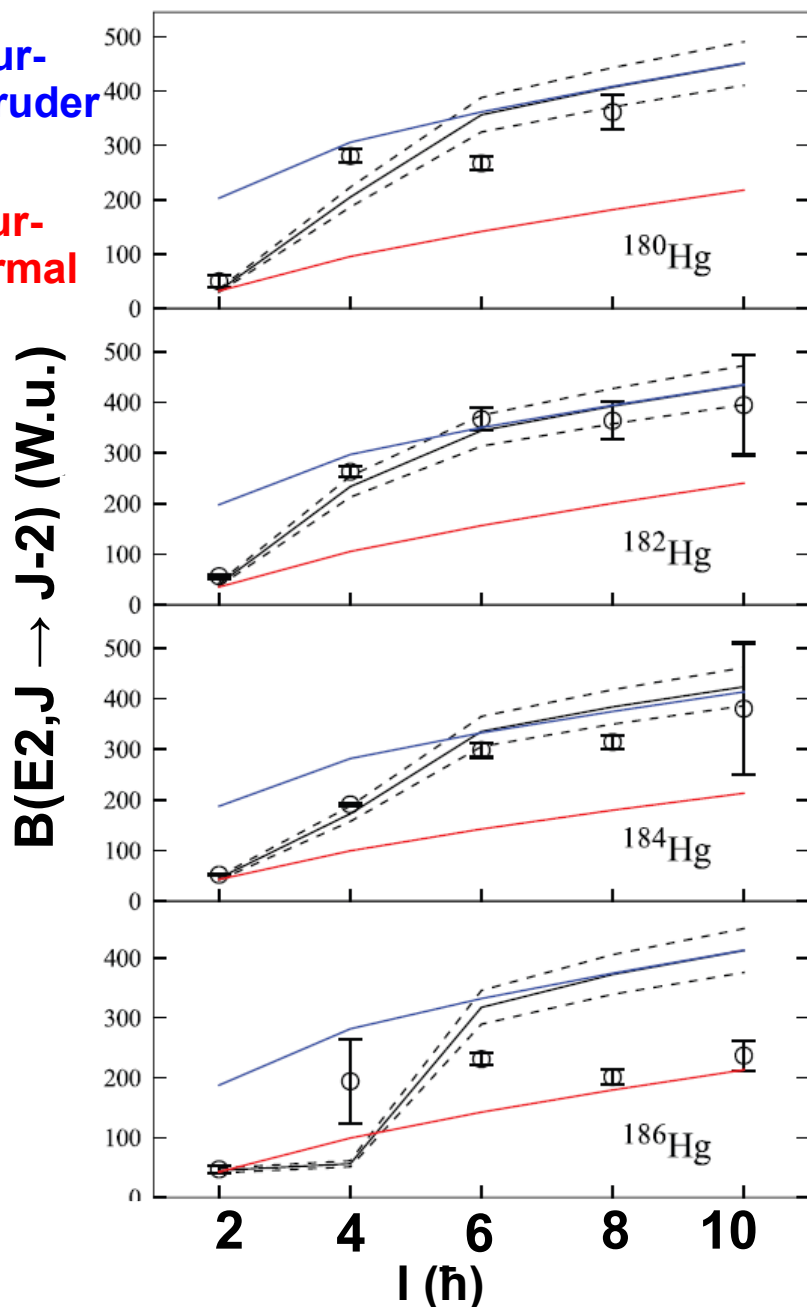


^{184}Hg , gate on shifted component
 $4_1^+ \rightarrow 2_1^+$

Shape coexistence in light Hg isotopes: band mixing in $^{180-186}\text{Hg}$

Unperturbed intruder

Unperturbed normal



Phenomenological two-band mixing calculations:
 → assume spin-independent interaction between two rotational structures
 → wave function amplitudes of two config. from mixing strengths (Lane et al., NPA 589, 129 (95))

			amplitude
^{182}Hg	$V = 89.4 \text{ keV}$	0	0.9606
		2	0.5382
	$E_0^n = 25.9 \text{ keV}$	4	0.1781
		6	0.1003
	$E_0^i = 309.0 \text{ keV}$	8	0.0697
	10	0.0534	
^{184}Hg	$V = 84.7 \text{ keV}$	0	0.9725
		2	0.7172
	$E_0^n = 20.4 \text{ keV}$	4	0.2014
		6	0.1025
	$E_0^i = 353.4 \text{ keV}$	8	0.0679
	10	0.0506	
^{186}Hg	$V = 66.3 \text{ keV}$	0	0.9915
		2	0.9506
	$E_0^n = 8.9 \text{ keV}$	4	0.2604
		6	0.0978
	$E_0^i = 505.4 \text{ keV}$	8	0.0587

Shape coexistence in light Hg isotopes

0_1^+ normal oblate configuration

2_1^+ strongly mixed in ^{182}Hg : 50% of each configuration
 ^{186}Hg : nearly pure normal configuration

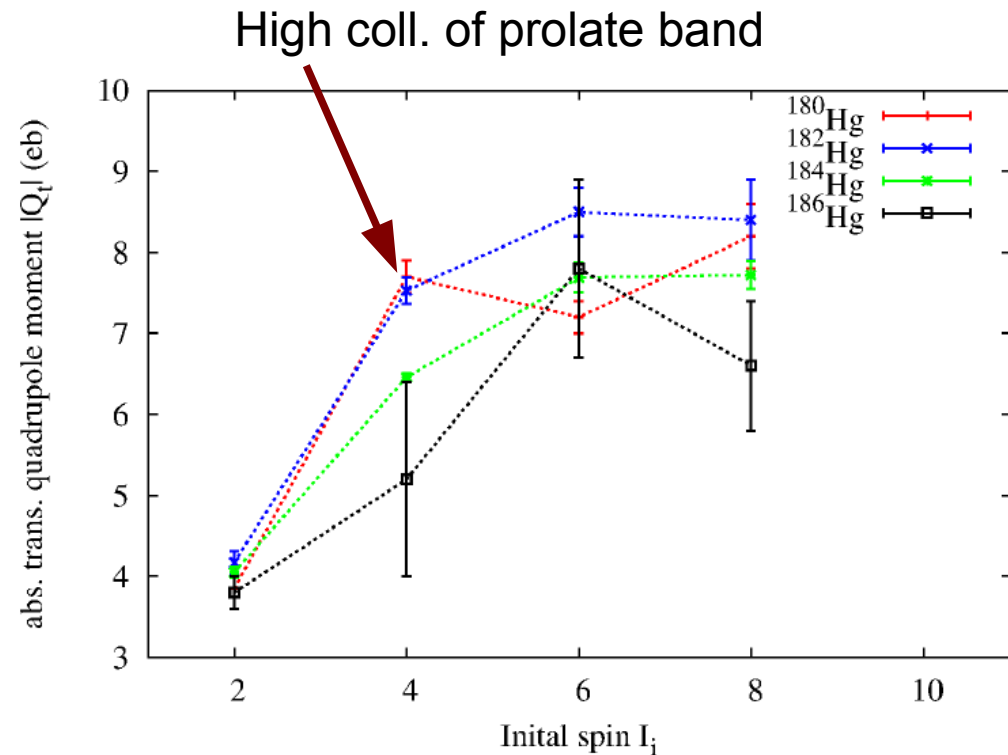
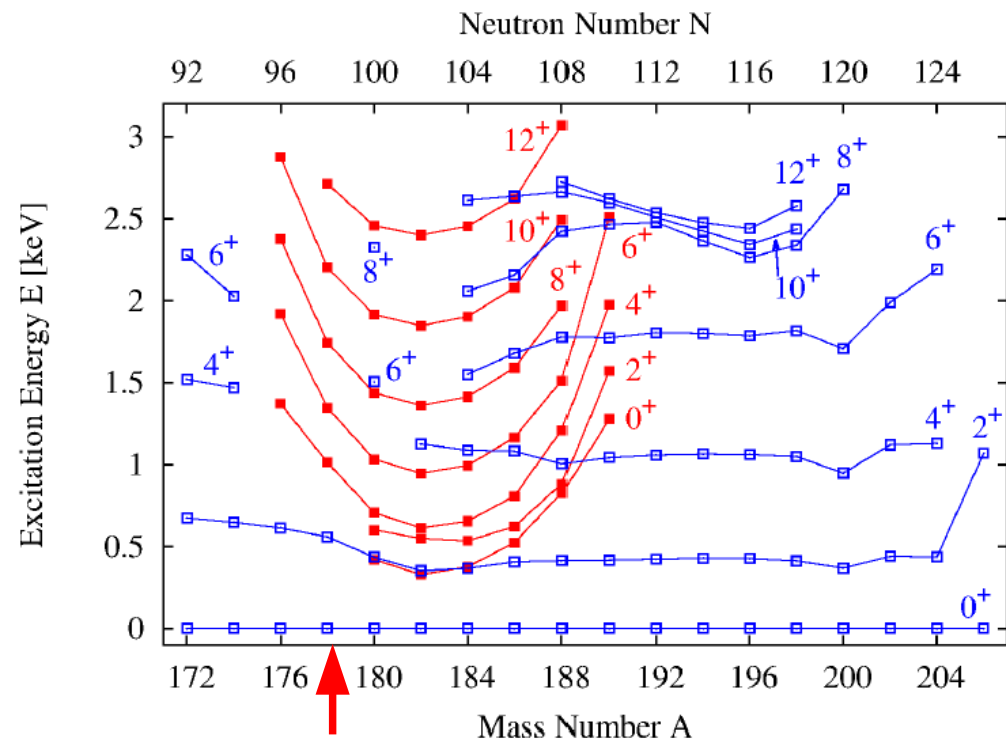
4_1^+ etc.: mainly prolate intruder configuration

L. Gaffney, M. Hackstein et al., PRC 89, 024307 (14)
Also confirmed in N. Bree et al., PRL 112, 162701 (14):
IBM based model, beyond mean field, two-state mixing

→ consistent with beyond mean field calculations
J.M. Yao, M. Bender, P.-H. Heenen, PRC 87, 034322 (12)

New experiments of our group:

1. Shape coexistence in ^{178}Hg



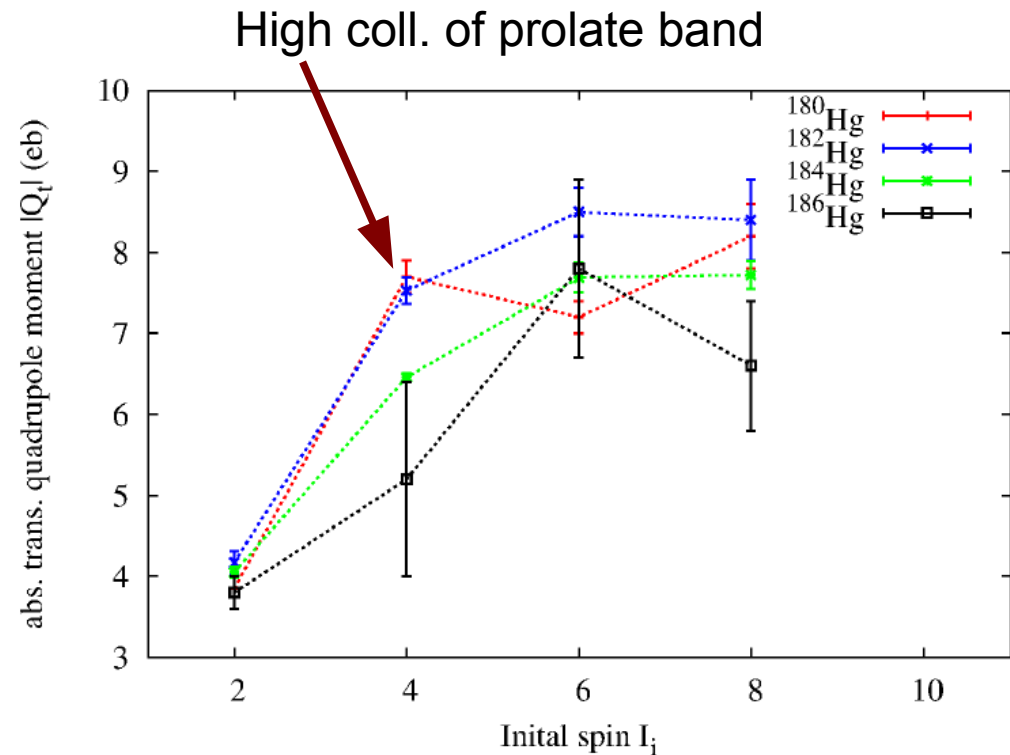
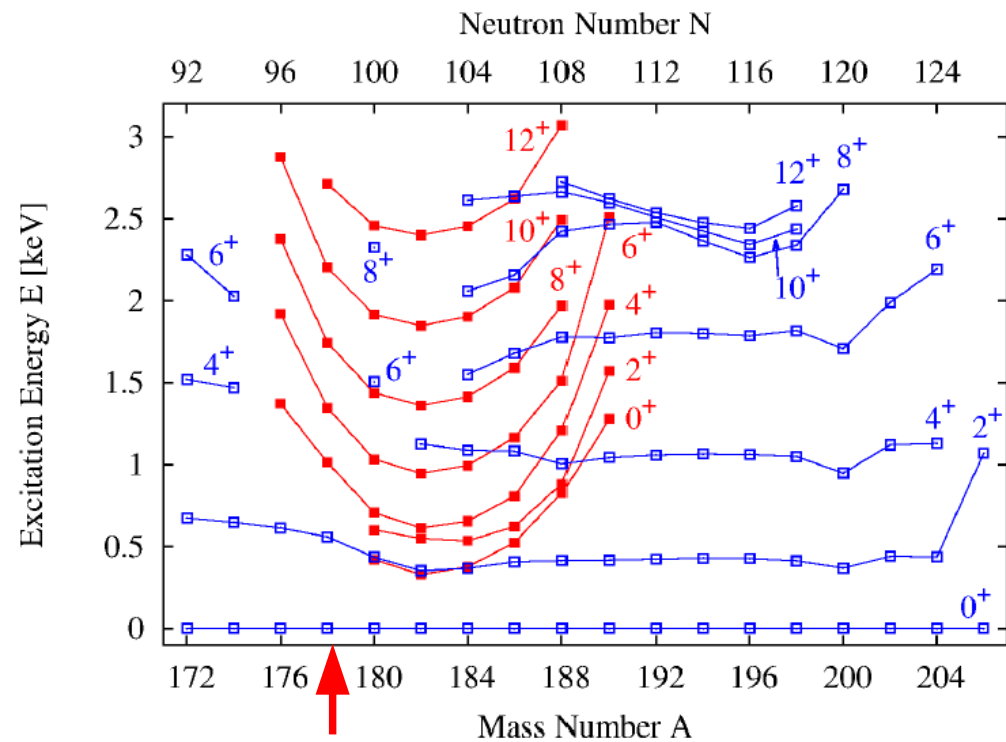
$^{180,182}\text{Hg}$: yrast E2 transition strengths from plunger exp. at JYFL using alpha-decay tagging (T. Grahn et al., PRC 80, 014324 (09))

→ 2_1^+ exhibit strong admixture of coexisting prolate and oblate structures

→ drop of Q_t of $2_1^+ \rightarrow 0_1^+$ as compared to $4_1^+ \rightarrow 2_1^+$ by factor of 2: weaker deformed oblate character of ground states.

New experiments of our group:

1. Shape coexistence in ^{178}Hg



^{178}Hg : no data on E2 transition strengths:

1. does parabolic trend continue?
 2. understand increase of $E(2_1^+)$
 3. assumption: transition towards near-spherical ground state
- M. Sandzelius et al., PRC 79, 064315 (09)

New experiments of our group:

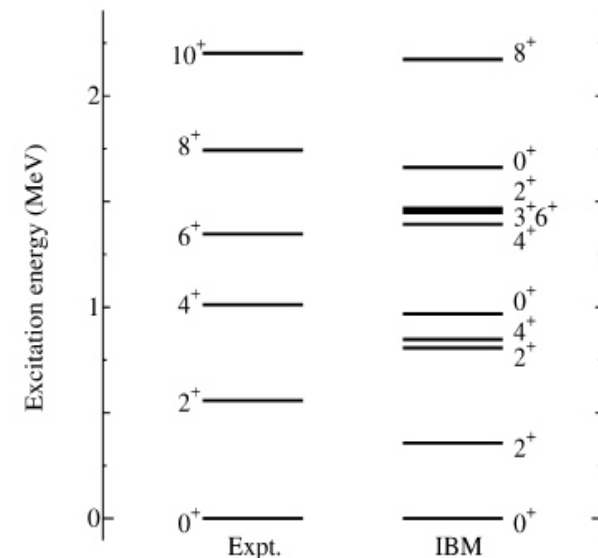
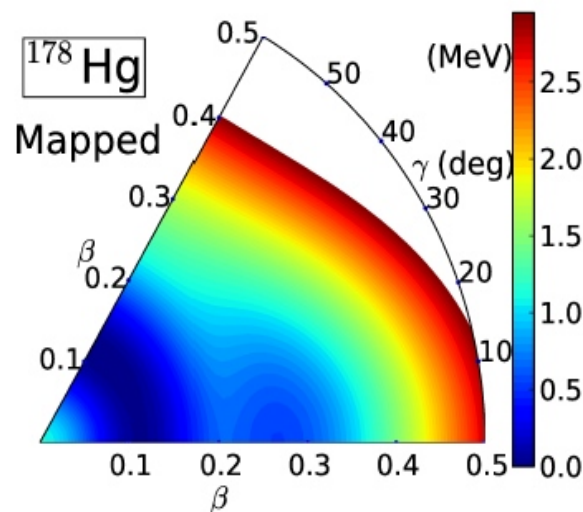
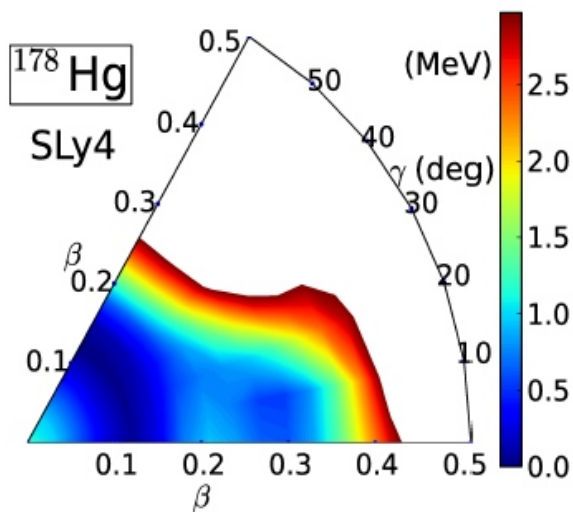
1. Shape coexistence in ^{178}Hg

Theoretical approach (K. Nomura):

mapping PES of mean-field model onto PES of IBM

→ successful for shape coexistence in n-deficient Pb isotopes

→ applied for ^{178}Hg :



→ 0_2^+ (2p,2h) configuration, prolate def.

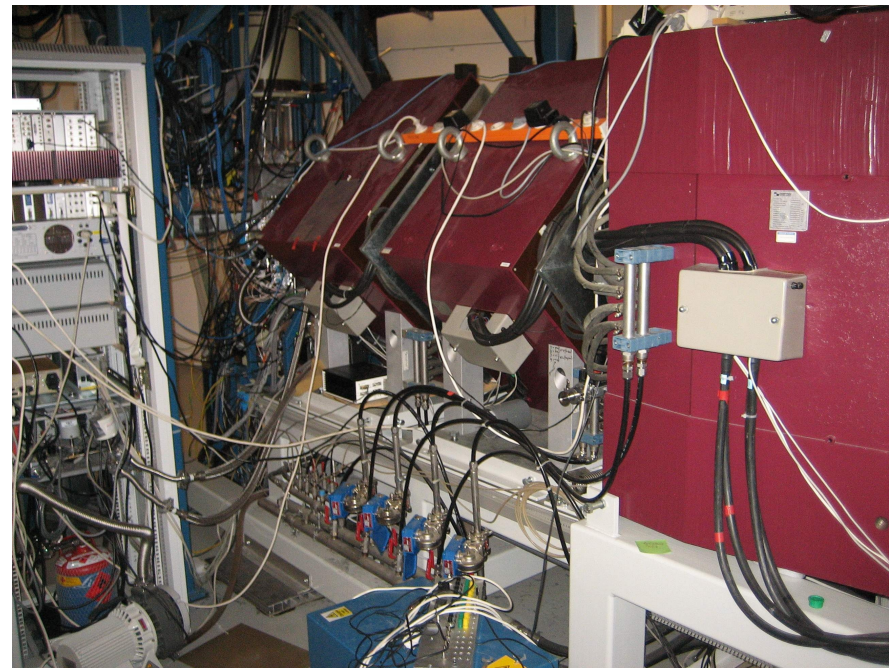
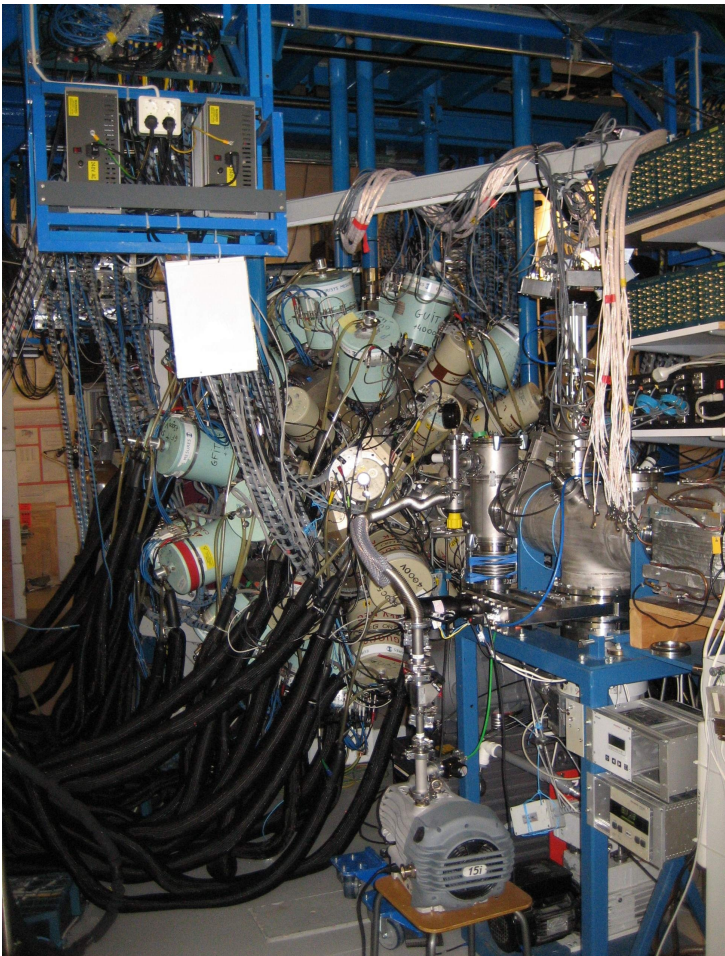
→ lowest yrast states: normal oblate / gamma-soft configuration

Measure yrast E2 transition strengths!

New experiments of our group:

1. Shape coexistence in ^{178}Hg

Experiment 07/2014 at JYFL: JUROGAM + DPUNS Plunger + RITU + α -decay tagging
 $^{103}\text{Rh}(^{78}\text{Kr}, p2n)^{178}\text{Hg}$ @ 351.5 MeV
Implantation rate GREAT ^{178}Hg : 0.35 /s
 $\sigma(^{178}\text{Hg}) = 50 \mu\text{barn}$ (Argonne)



RITU + GREAT

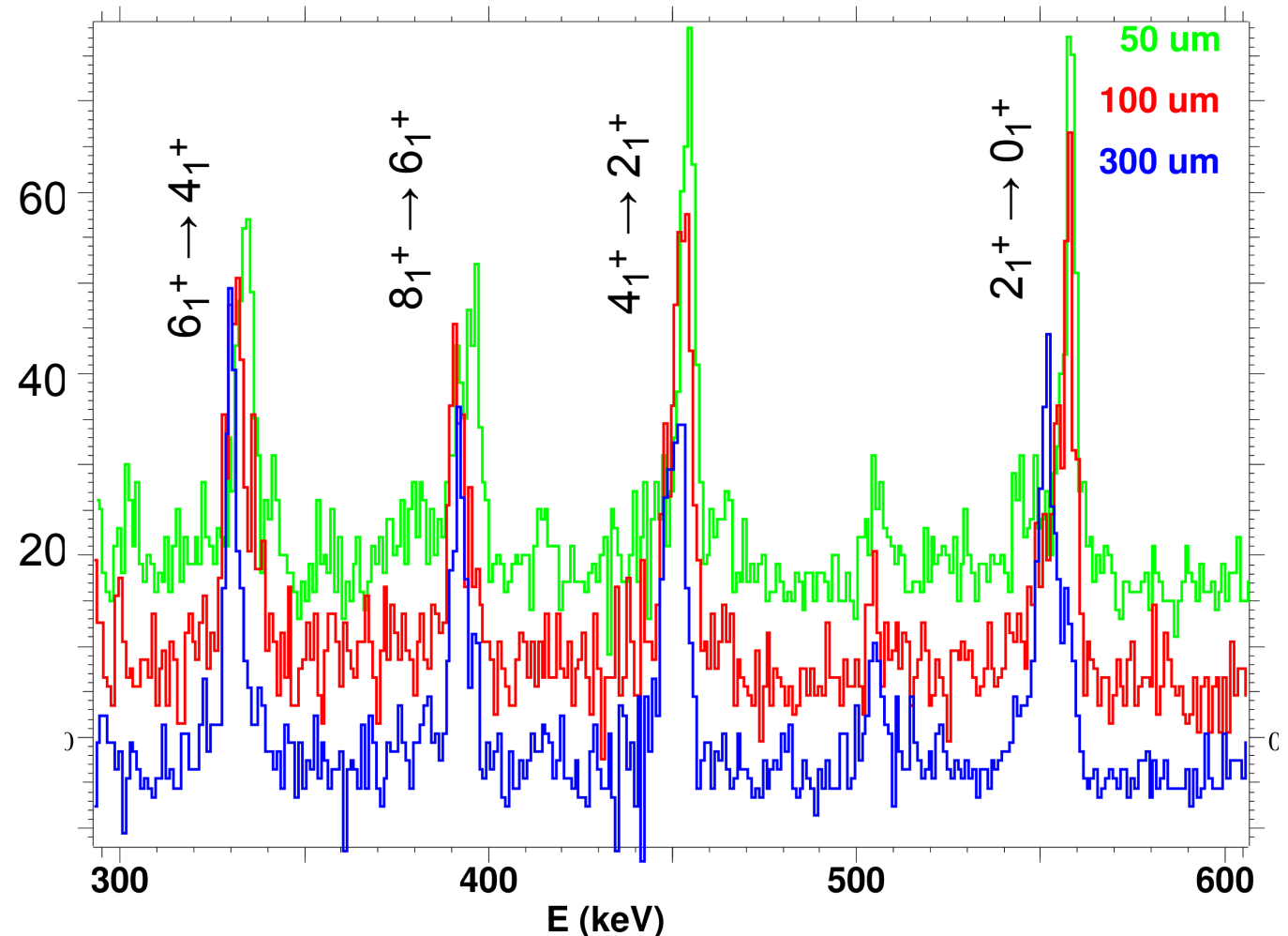
JUROGAM II + DPUNS Plunger

New experiments of our group: 1. Shape coexistence in ^{178}Hg

Experiment 07/2014 at JYFL: JUROGAM + DPUNS Plunger + RITU + α -decay tagging
 $^{103}\text{Rh}(^{78}\text{Kr}, p2n)^{178}\text{Hg}$ @ 351.5 MeV
Implantation rate GREAT ^{178}Hg : 0.35 /s

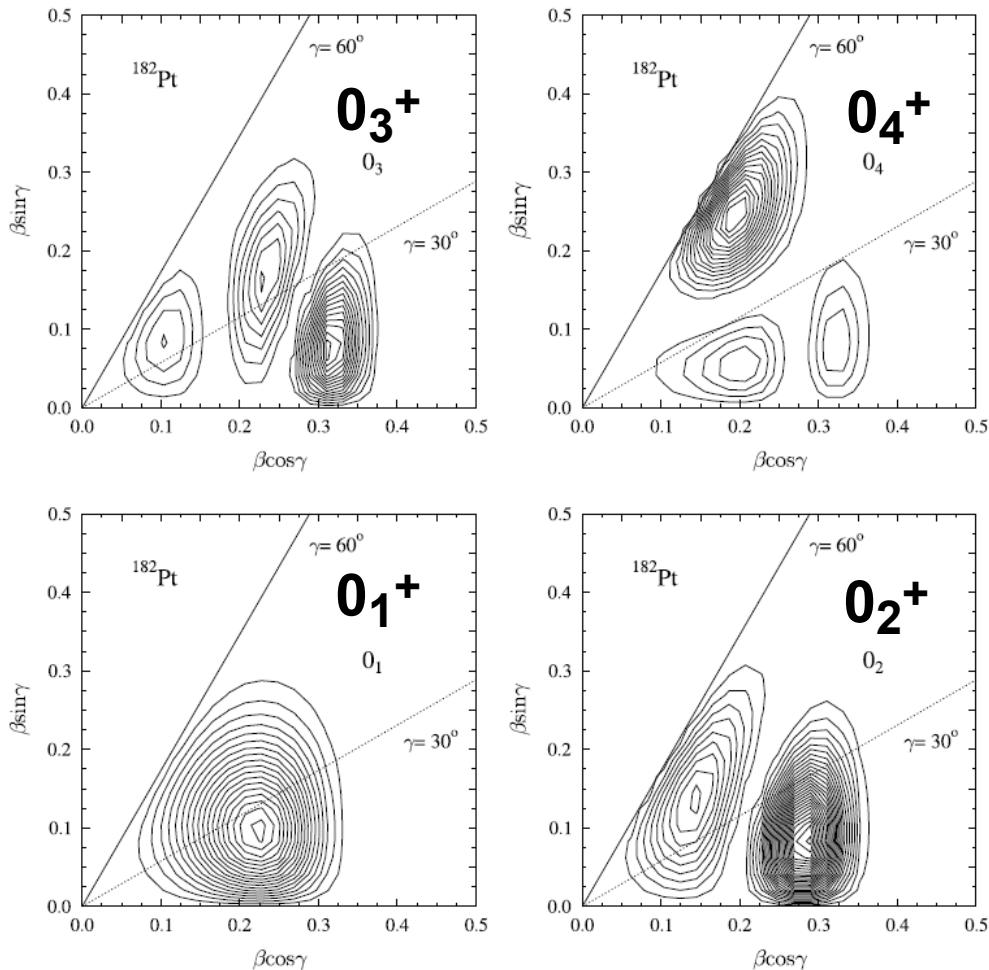
α -tagged spectrum ^{178}Hg

→ data analysis
under work...



New experiments of our group:

2. Shape coexistence in ^{180}Pt



→ **Plunger experiment at JYFL:**
 Cologne Plunger + JUROGAM II
 $^{98}\text{Mo}(^{86}\text{Kr}, 4n)^{180}\text{Pt}$ @ 364 MeV
 → lifetimes of 4_1^+ , 6_1^+ , 8_1^+

→ **fast timing experiment at IKP Cologne**
 HORUS spectrometer with 6 $\text{LaBr}_3(\text{Ce})$
 detectors with BGO shields,
 8 HPGe detectors
 $^{168}\text{Yb}(^{16}\text{O}, 4n)^{180}\text{Pt}$ @ 88 MeV
 → lifetimes of 2_1^+ , 4_1^+

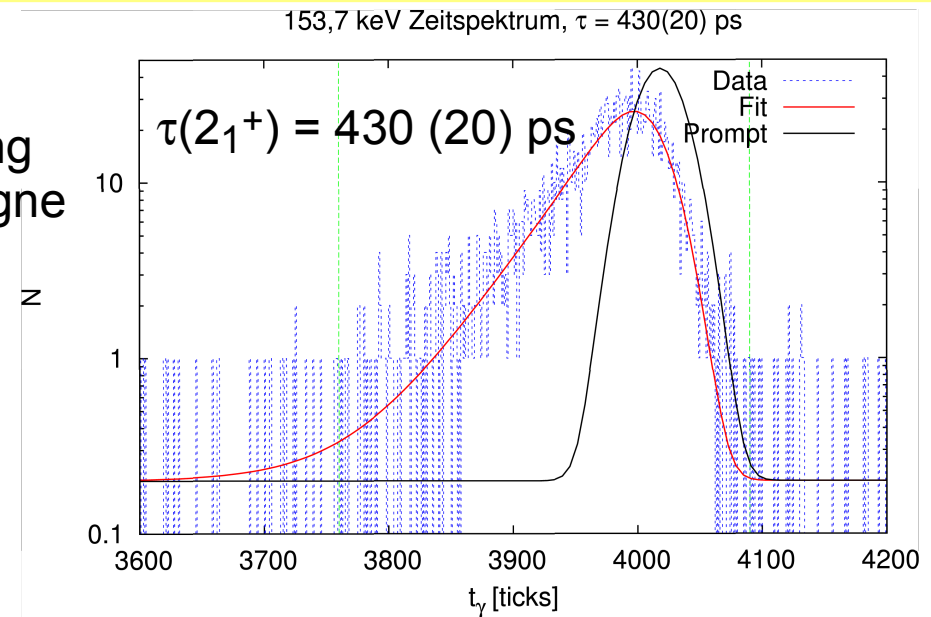
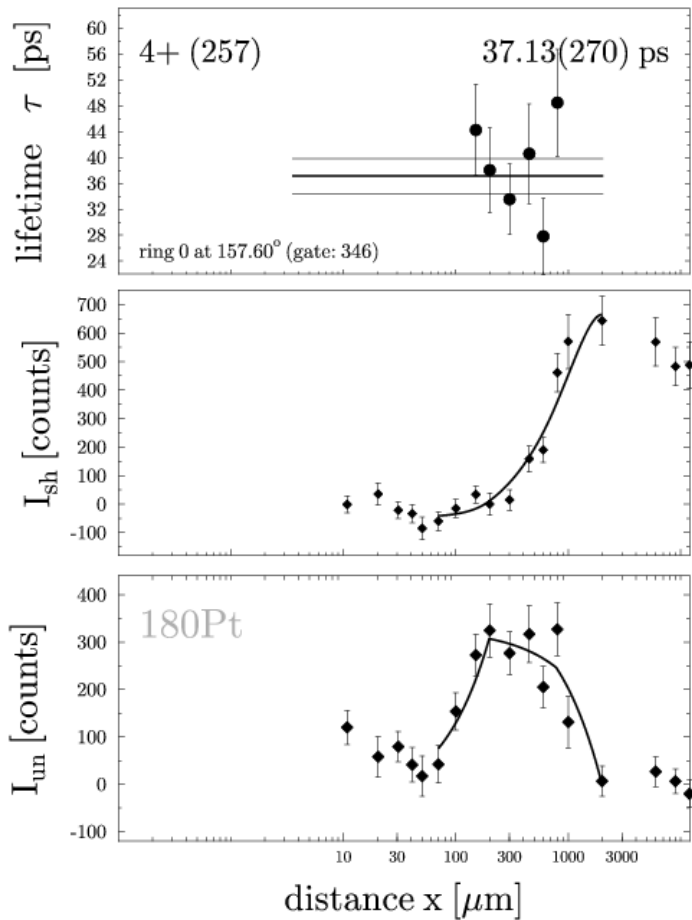
GCM calculations for ^{182}Pt
 K.A. Gladnishki, NPA 877, 19 (12)

New experiments of our group: 2. Shape coexistence in ^{180}Pt

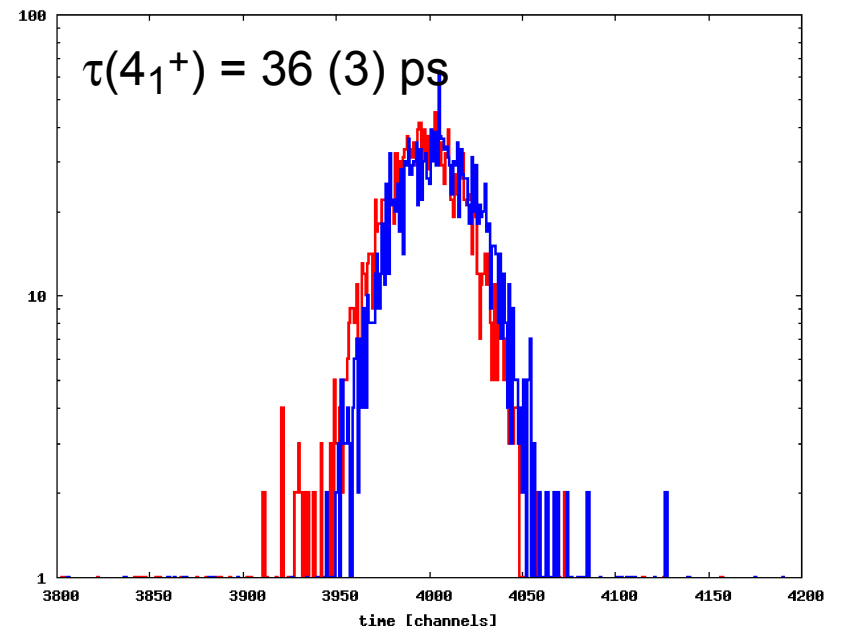
Preliminary results
C. Müller-Gatermann

Plunger experiment JYFL
 $\tau(4_1^+) = 37.1 (27) \text{ ps}$

Fast timing
IKP Cologne



GCD
method



Outline

1. Introduction
2. The plunger technique
3. Other lifetime techniques used by our group:
 - a. Fast timing
 - b. Doppler-shift attenuation method
4. Shape coexistence in neutron deficient Hg isotopes
5. Critical point symmetries in the $A=180$ mass region
6. Search for isovector excitations in the vicinity of ^{208}Pb

Motivation: critical point symmetries in A=180 region?

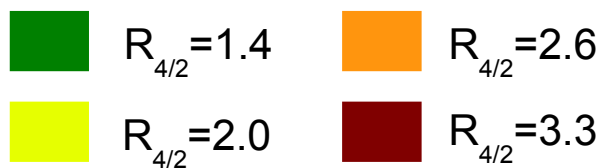
→ $^{176,178}\text{Os}$: candidates for nuclei at critical point of spherical – rotor shape phase transition

A. Dewald et al., J. Phys. G 31, S1427 (05)

→ other approaches: - IBM
- GCM

→ Prediction of an oblate-prolate shape coexistence

→ measure precisely yrast $B(E2)$ values in ^{180}Os for the first time



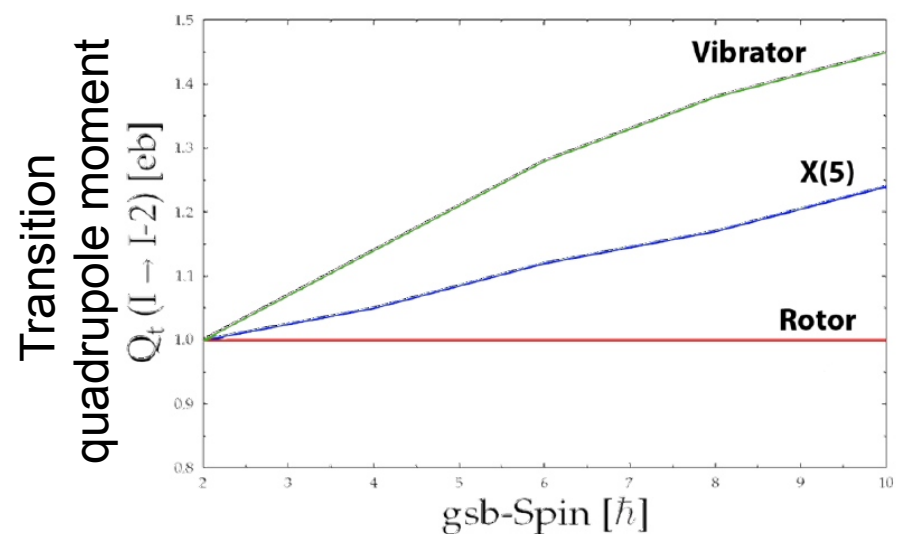
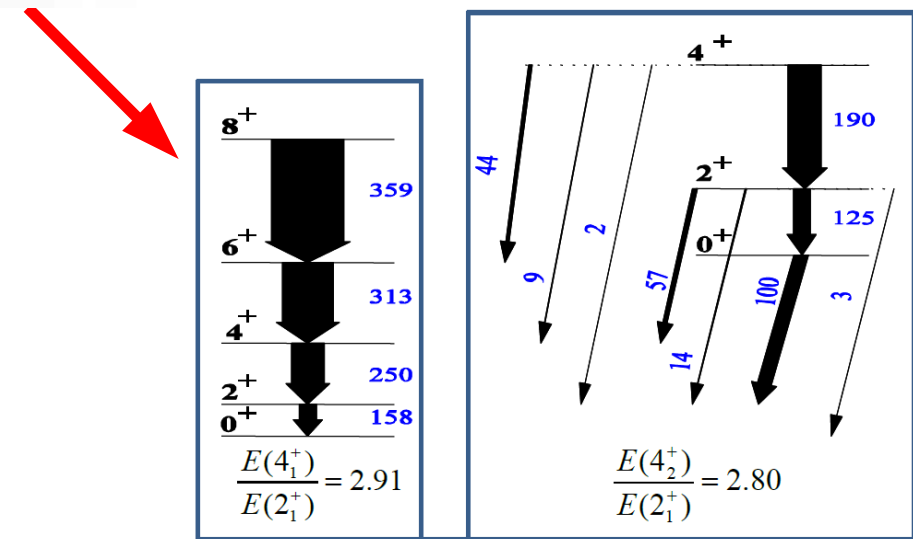
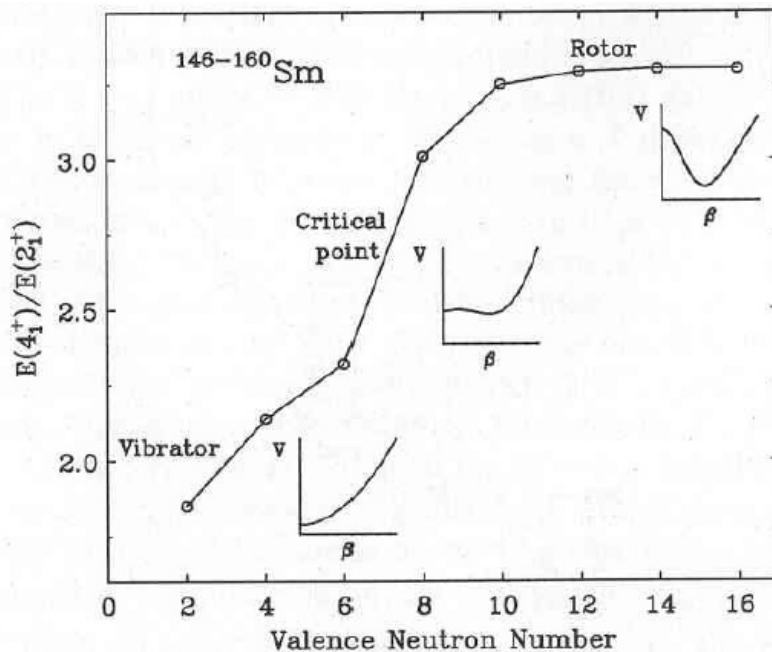
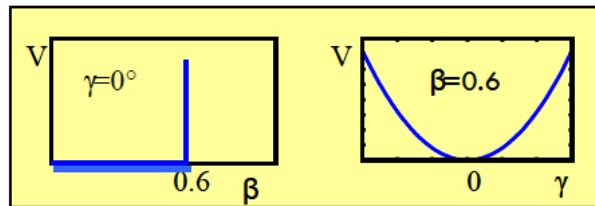
Z=82

^{180}Os

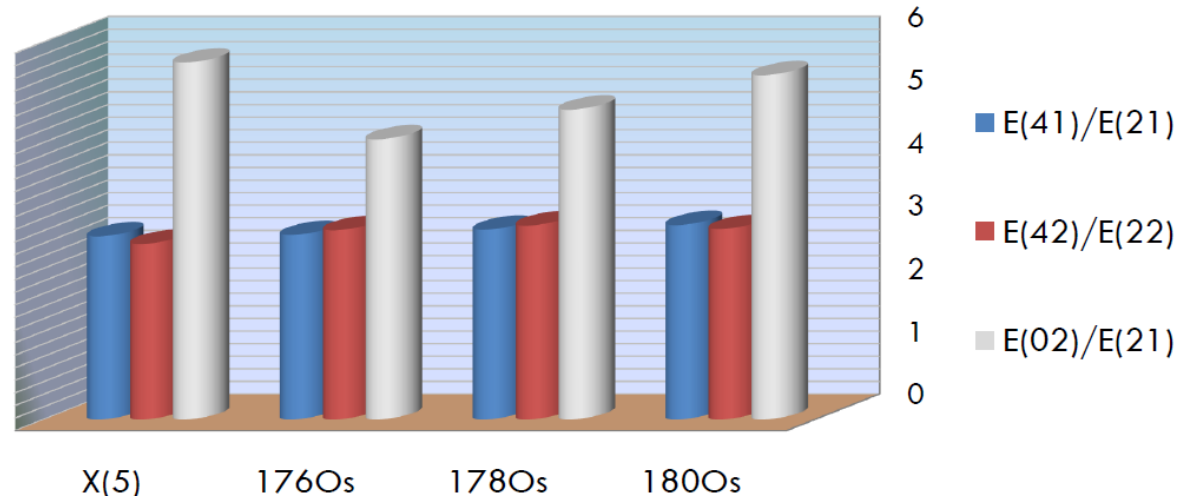
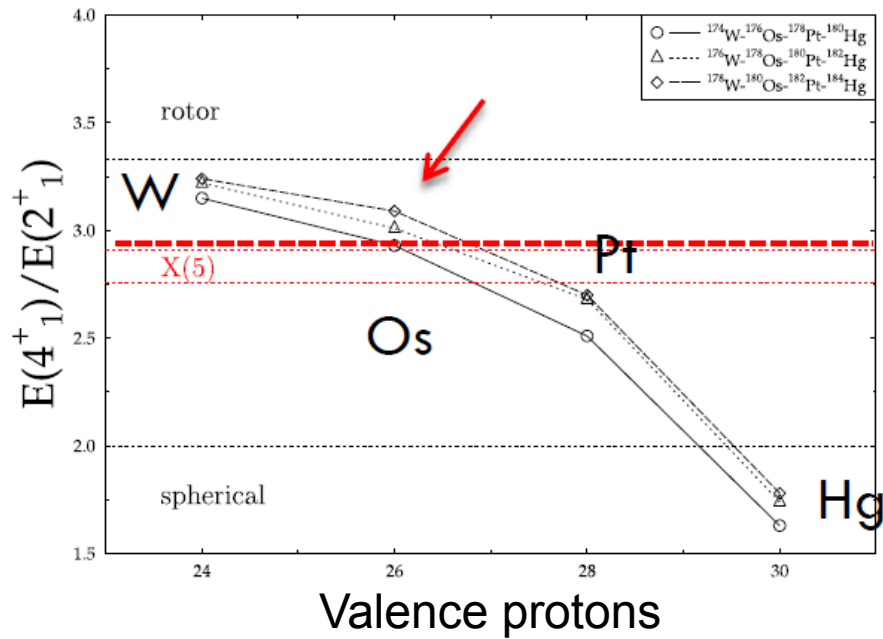
Z	178Pb	179Pb	180Pb	181Pb	182Pb	183Pb	184Pb	185Pb	186Pb	187Pb	188Pb	189Pb	190Pb	191Pb	192Pb	193Pb	194Pb
82	177Tl	178Tl	179Tl	180Tl	181Tl	182Tl	183Tl	184Tl	185Tl	186Tl	187Tl	188Tl	189Tl	190Tl	191Tl	192Tl	193Tl
80	176Hg	177Hg	178Hg	179Hg	180Hg	181Hg	182Hg	183Hg	184Hg	185Hg	186Hg	187Hg	188Hg	189Hg	190Hg	191Hg	192Hg
78	175Au	176Au	177Au	178Au	179Au	180Au	181Au	182Au	183Au	184Au	185Au	186Au	187Au	188Au	189Au	190Au	191Au
76	174Pt	175Pt	176Pt	177Pt	178Pt	179Pt	180Pt	181Pt	182Pt	183Pt	184Pt	185Pt	186Pt	187Pt	188Pt	189Pt	190Pt
74	173Ir	174Ir	175Ir	176Ir	177Ir	178Ir	179Ir	180Ir	181Ir	182Ir	183Ir	184Ir	185Ir	186Ir	187Ir	188Ir	189Ir
	172Os	173Os	174Os	175Os	176Os	177Os	178Os	179Os	180Os	181Os	182Os	183Os	184Os	185Os	186Os	187Os	188Os
	171Re	172Re	173Re	174Re	175Re	176Re	177Re	178Re	179Re	180Re	181Re	182Re	183Re	184Re	185Re	186Re	187Re
	170W	171W	172W	173W	174W	175W	176W	177W	178W	179W	180W	181W	182W	183W	184W	185W	186W
	96	98	100	102	104	106	108	110	N								

Motivation: X(5)

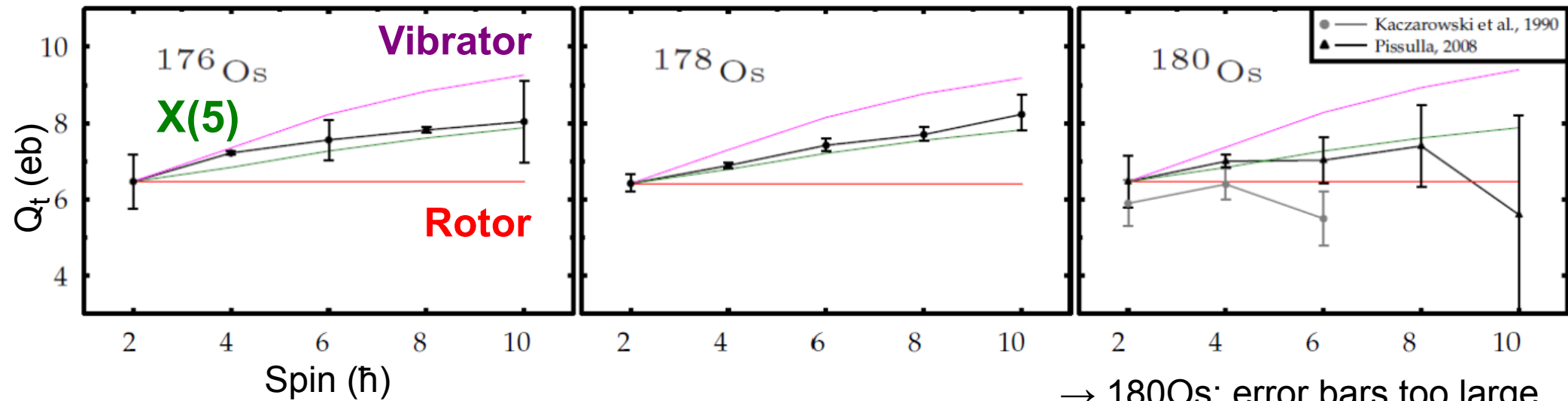
- F. Iachello, Phys. Rev. Lett. 87, 052502 (2001)
- X(5): critical point of the spherical – rotor shape phase transition
- Analytic solution of Bohr hamiltonian with square well potential for β
- Experimental signatures: **E2 strengths, level scheme**



X(5) properties in A=180 region



Transition quadrupol moments in yrast band:

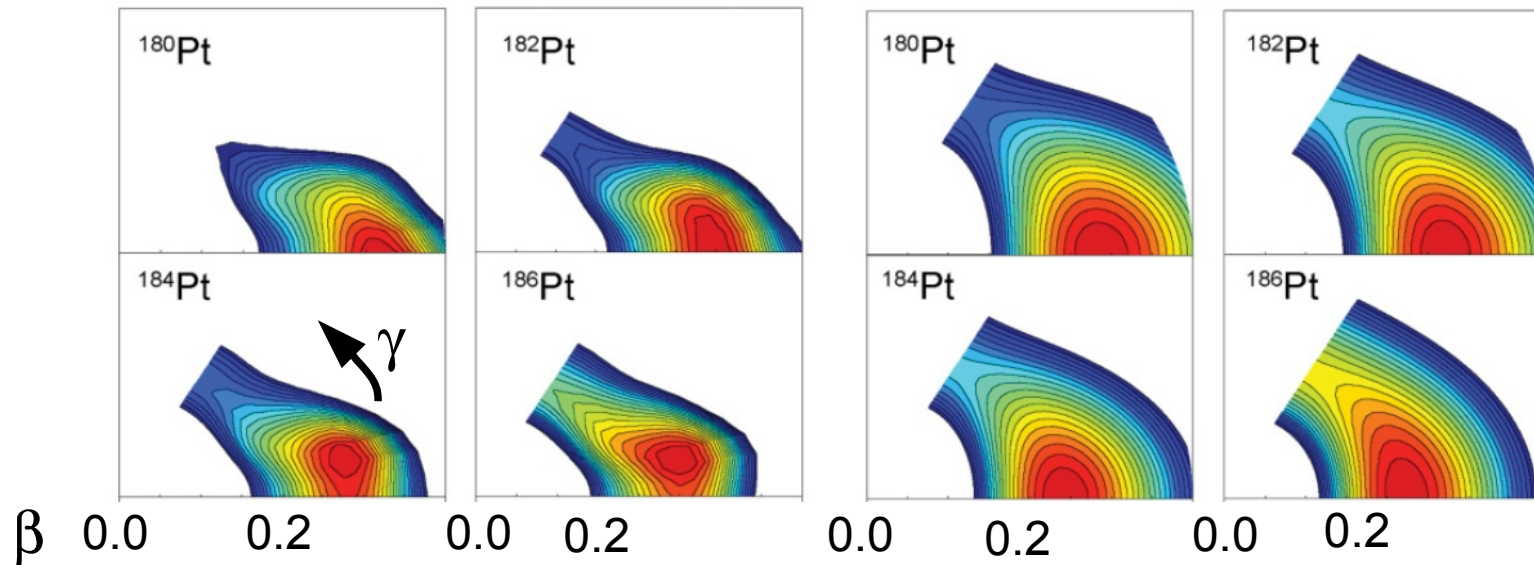


→ ^{180}Os : error bars too large.

Oblate-prolate shape coexistence around ^{180}Os ?

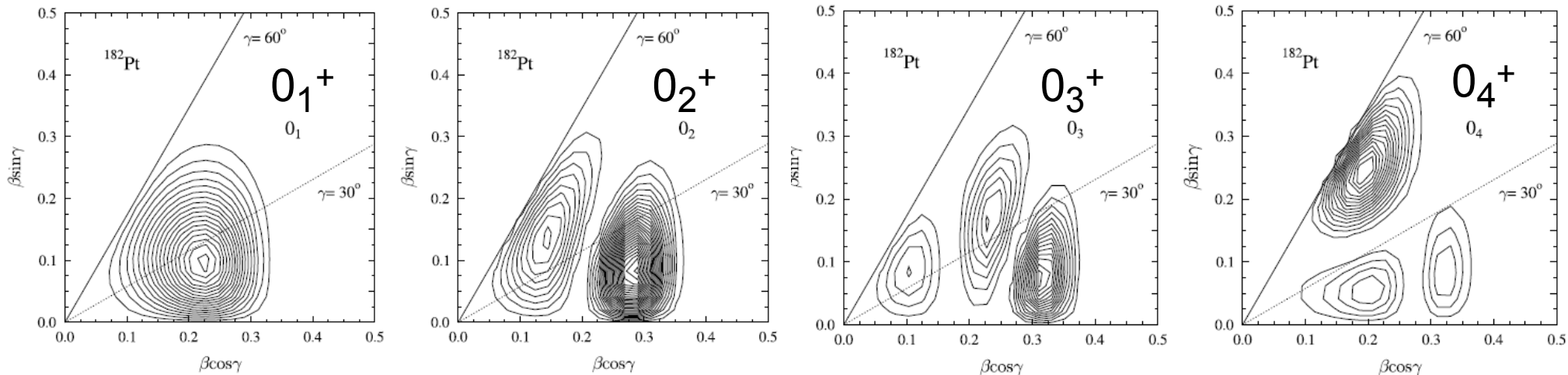
Potential Energy Surfaces (HFB)

Potential Energy Surfaces (IBM)



180-186Pt:
prolate minimum,
oblate saddle point
K. Nomura et al.,
PRC 83, 014309 (2011)

General collective model: PES for $0_1^+ - 0_4^+$ states in ^{182}Pt : multi component structure
 0_4^+ nearly oblate (K. Gladnishki et al., NPA 877, 19 (2012)) \rightarrow ^{180}Os ?



Experiment an ^{180}Os

Cologne plunger at GASP-II, INFN, Legnaro

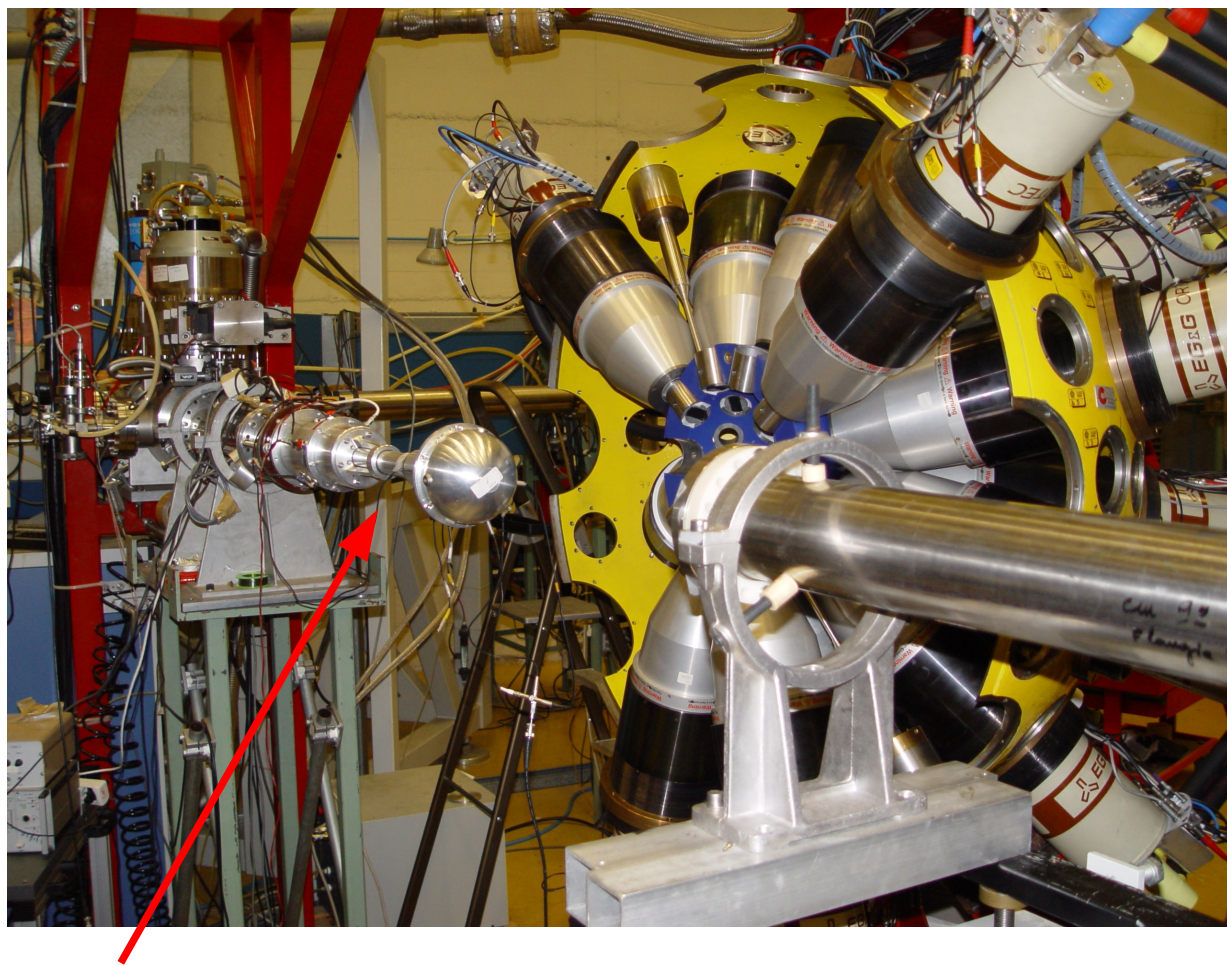
Reaction: $^{150}\text{Nd}(^{36}\text{S},6n)^{180}\text{Os}$
 $^{150}\text{Nd}(^{36}\text{S},5n)^{181}\text{Os}$

Beam $E(^{36}\text{S})=185\text{ MeV}$

Target: $2\text{ mg/cm}^2\ ^{150}\text{Nd}$
on $2.2\text{ mg/cm}^2\ \text{Ta}$

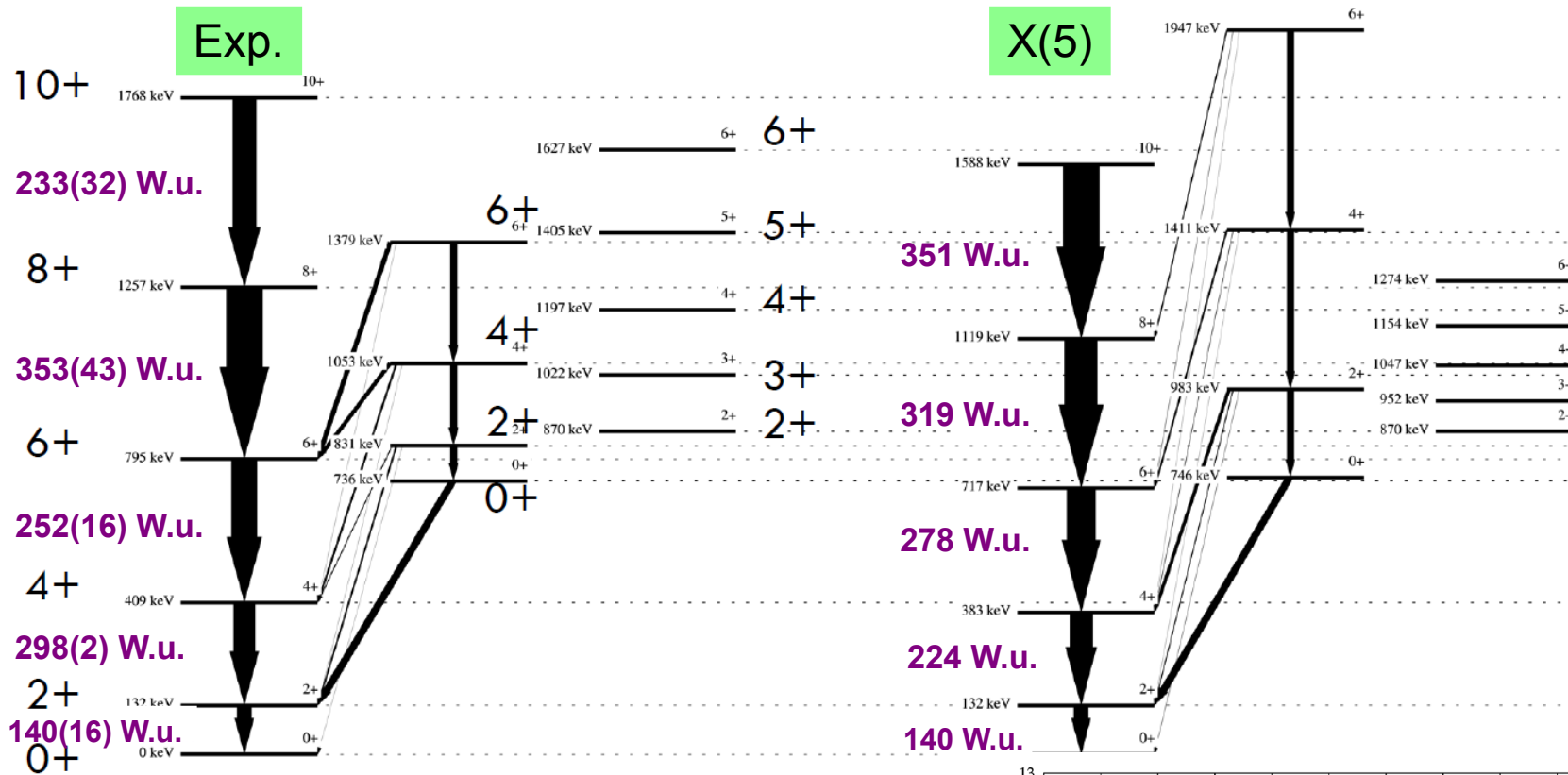
Stopper: $10.7\text{ mg/cm}^2\ \text{Au}$
 $v/c = 1.78(4)\%$

Lifetimes of yrast states up to 16_1^+
7 lifetimes of negative parity states

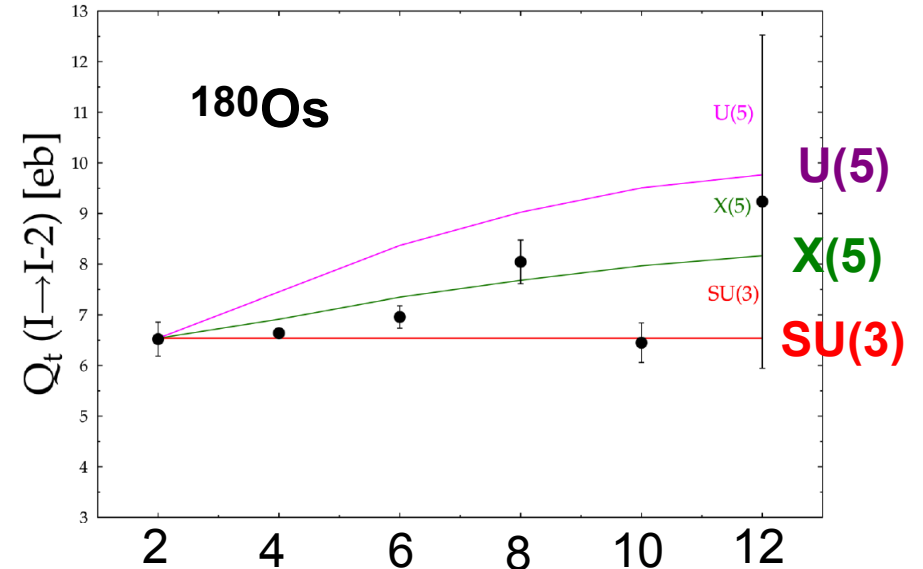
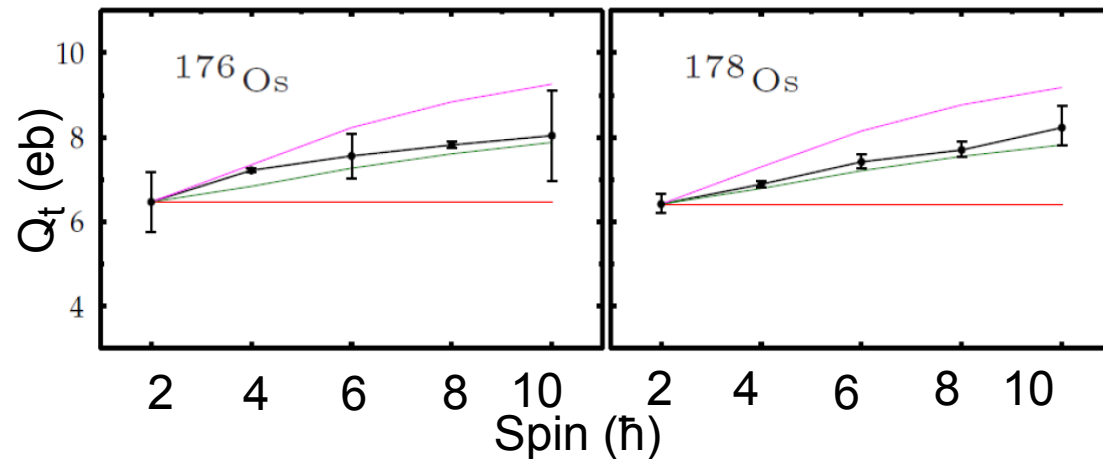


Cologne plunger

180Os: X(5) properties?



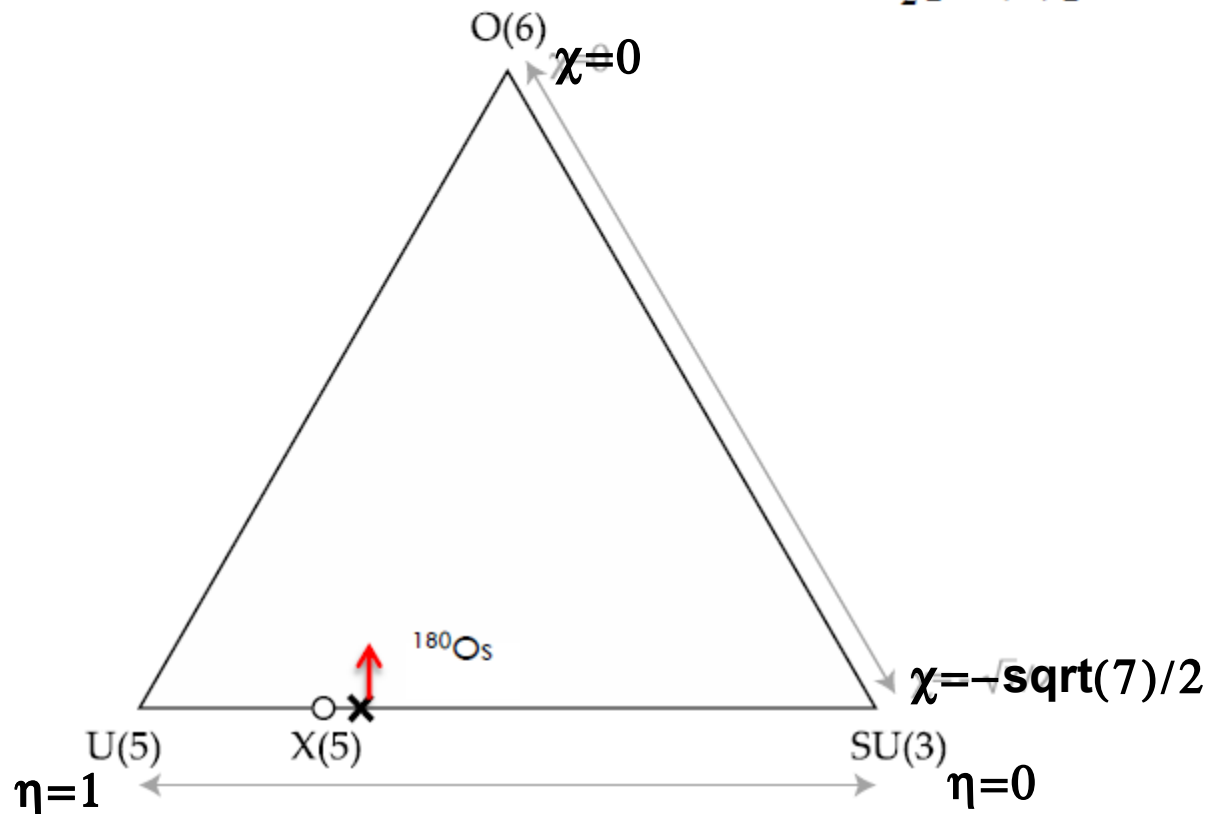
Transition quadrupole moments



^{180}Os in the IBM

- Fit in IBM in transition $U(5) - SU(3)$ ($\chi = -\sqrt{7}/2$):
No sufficient description of interband transition strength ratios
 $l_\beta \rightarrow l_g, l_\beta \rightarrow (l+2)_g$
- use $O(6)$ admixture, i.e., $\chi > -\sqrt{7}/2$
vary η, χ for best reproduction of relative yrast $B(E2)$ values

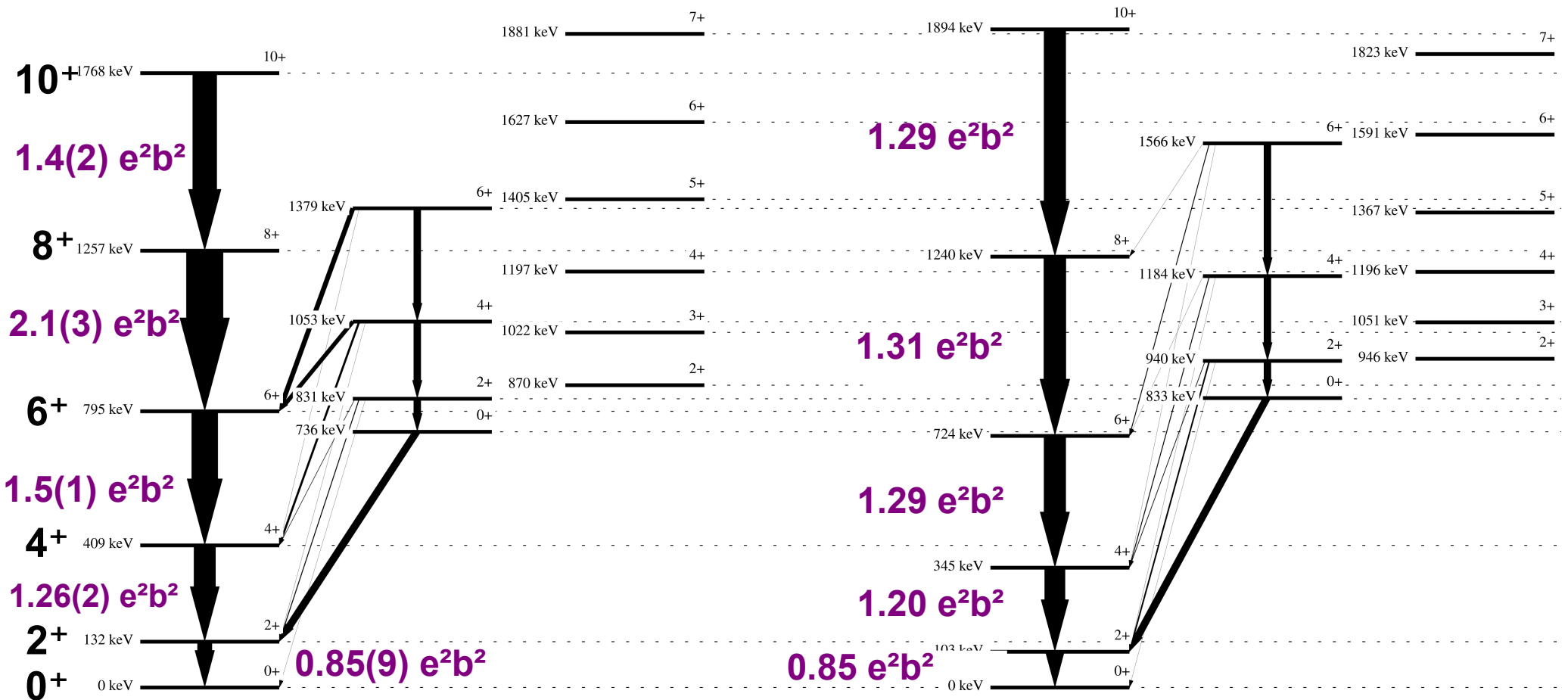
$$H = \varepsilon C_1[U(5)] + \delta C_2[SU(3)] + \gamma C_2[O(3)] + \alpha C_2[O(6)]$$



^{180}Os in the IBM

Exp

IBM



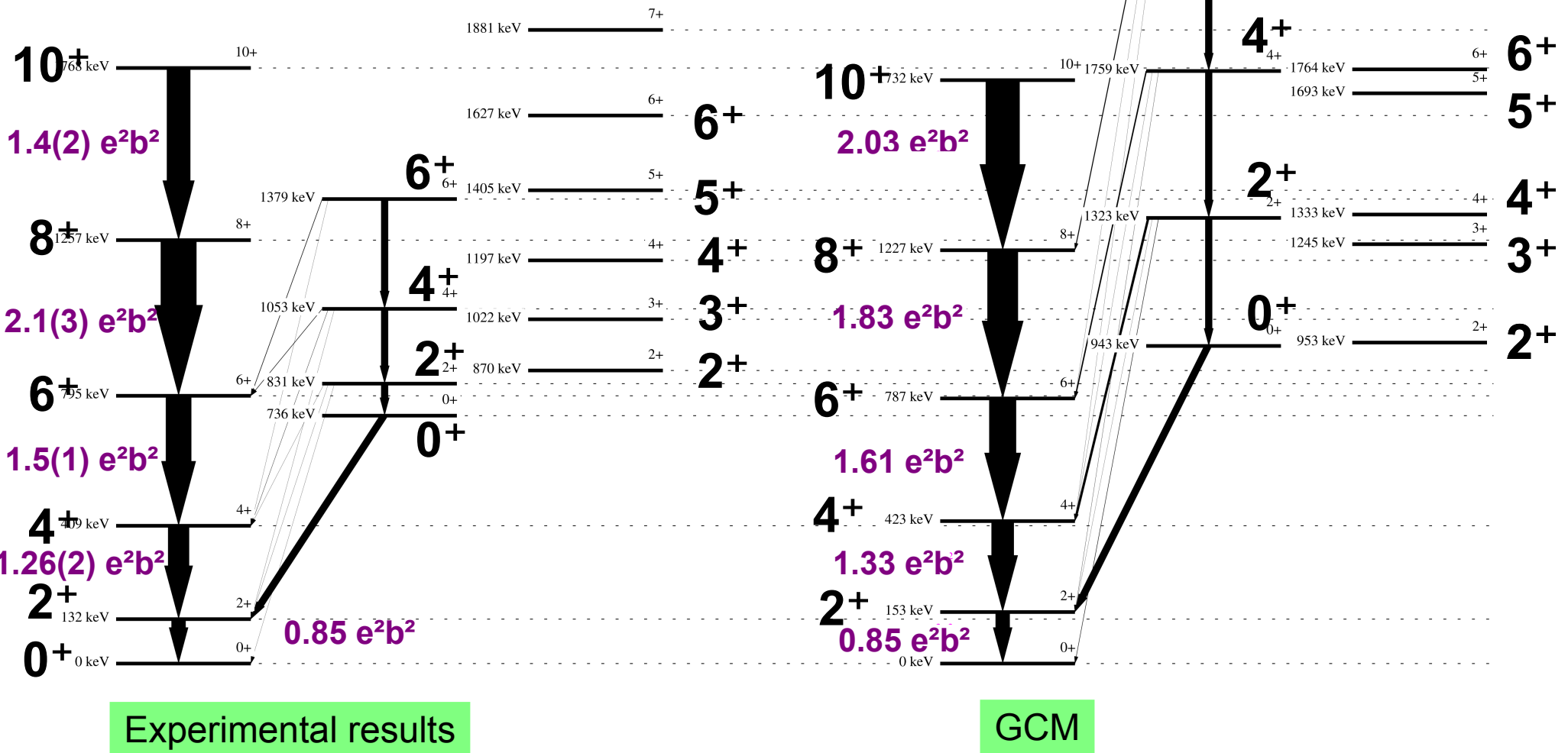
IBM in transition U(5) – SU(3) with small O(6) contribution: good description of exp. data

^{180}Os in the General Collective Model (P. Petkov)

GCM: Quadrupole surface oscillations

$$R(\theta, \phi) = R_0 \left(1 + \sum_{\mu} \alpha_{2\mu}^* Y_{2\mu}(\theta, \phi) \right)$$

Fit using E_{level} , $B(E2)$, Q_t



Experimental results

GCM

Results 180Os

- Lower yrast states can be described with X(5)
- IBM in transition U(5) – SU(3) with small O(6) admixture results in reasonable description
- GCM describes yrast states well.
Predictions of GCM hint for shape shape coexistence,
e.g. prediction of gamma-soft 0_3^+ (not observed)
 0_2^+ prolate def.

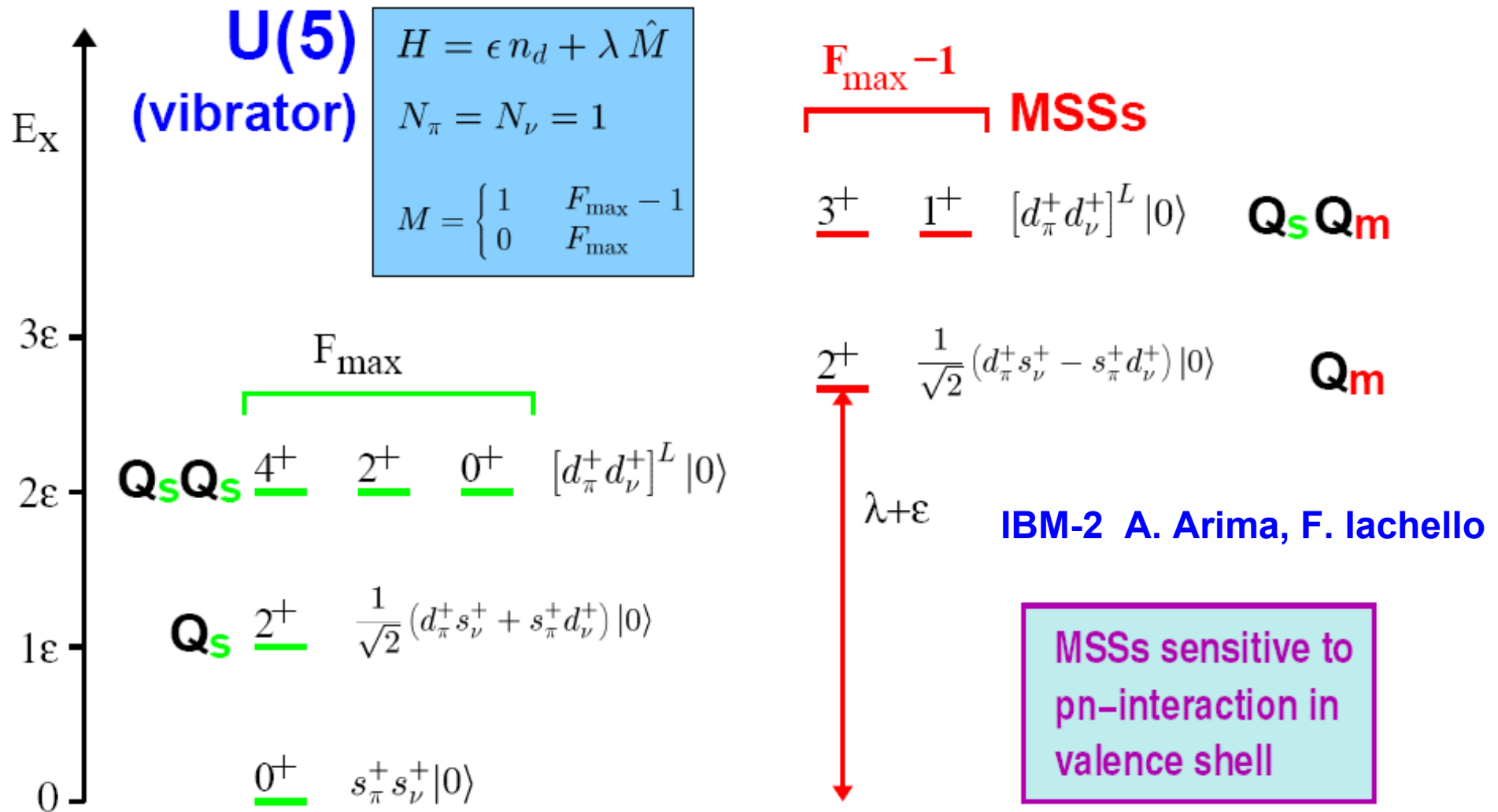
Outline

1. Introduction
2. The plunger technique
3. Other lifetime techniques used by our group:
 - a. Fast timing
 - b. Doppler-shift attenuation method
4. Shape coexistence in neutron deficient Hg isotopes
5. Critical point symmetries in the $A=180$ mass region
6. Search for isovector excitations in the vicinity of ^{208}Pb

Definition of mixed-symmetry states

One-phonon $2^+_{1,ms}$ fundamental quadrupole-collective isovector excitation in the valence shell for spherical vibrational nuclei

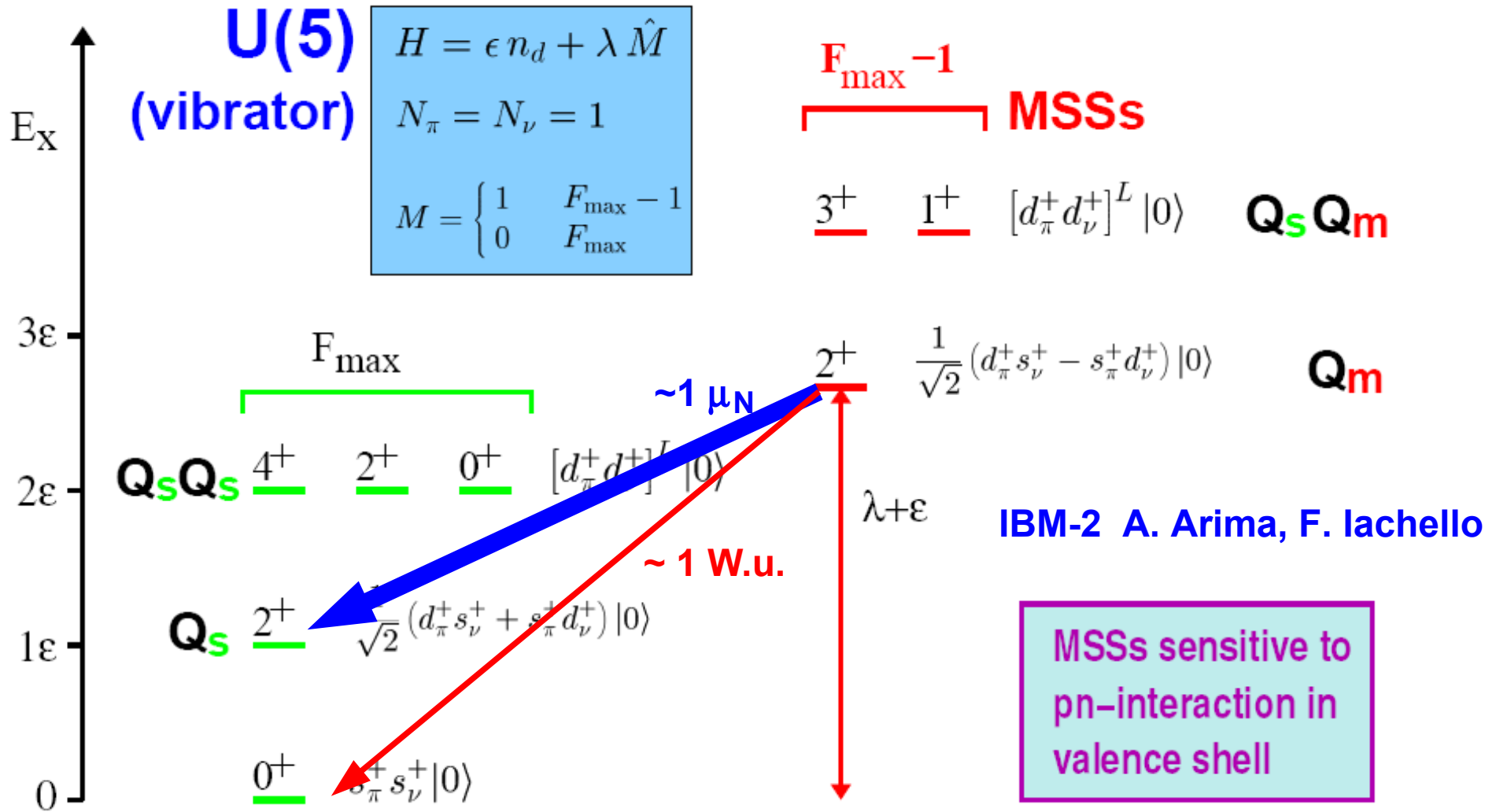
Simple Example: Harmonic Oscillator, N=2



Definition of mixed-symmetry states

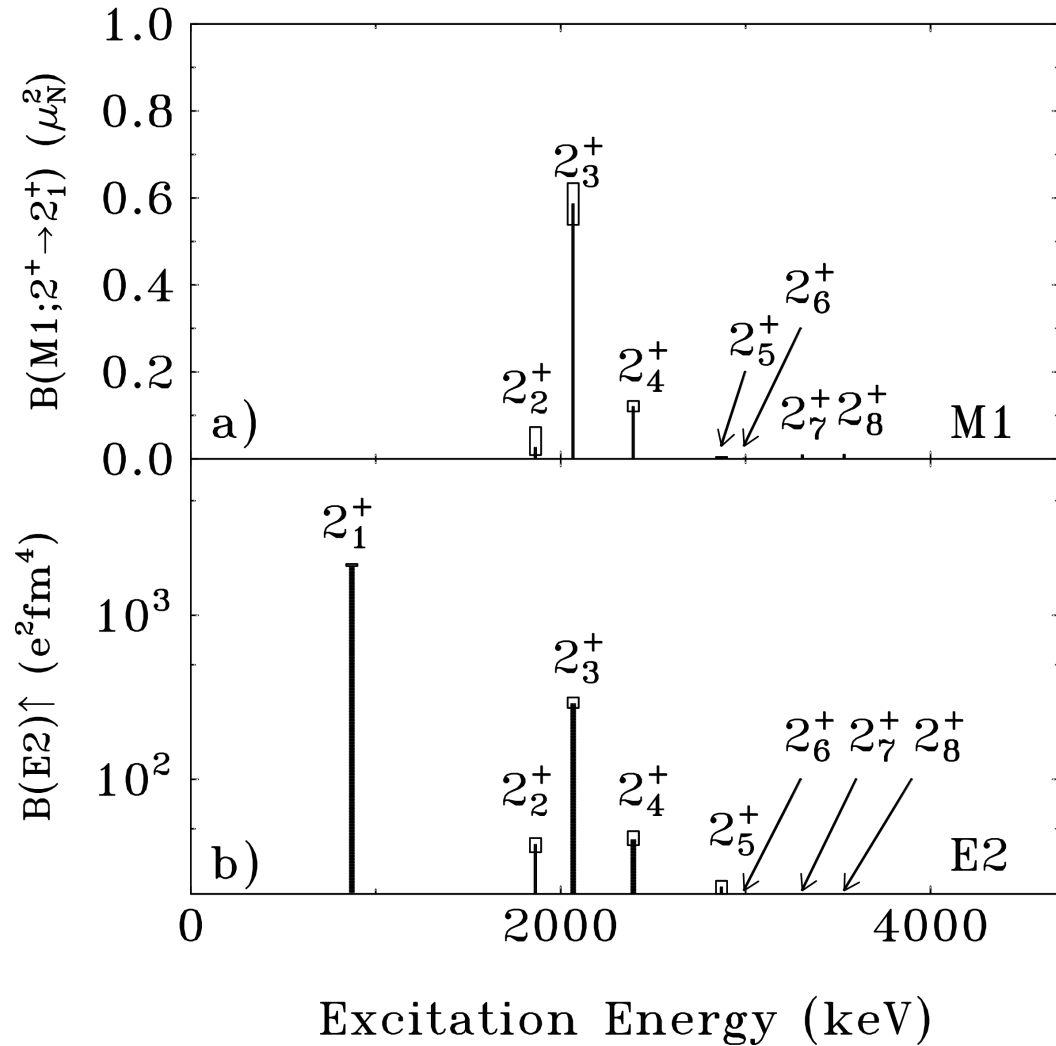
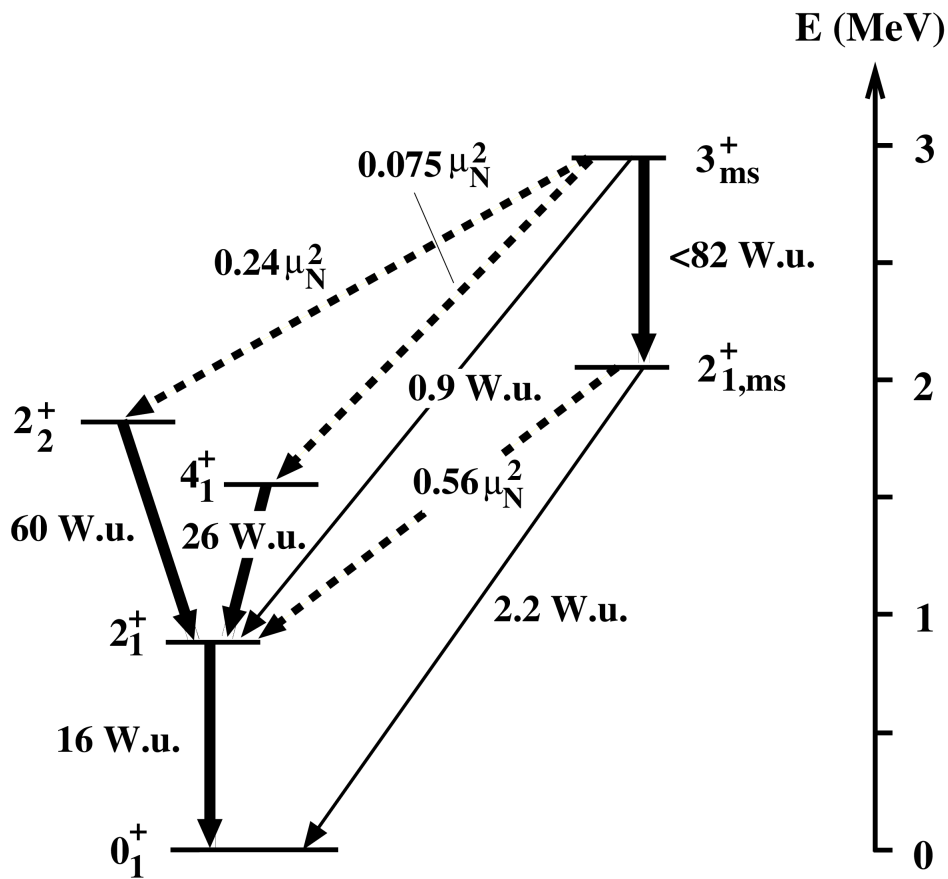
One-phonon $2^+_{1,ms}$ fundamental quadrupole-collective isovector excitation in the valence shell for spherical vibrational nuclei

Simple Example: Harmonic Oscillator, N=2



Best case so far: ^{94}Mo

^{94}Mo (vibrator-like): $2_{1,ms}^+$ and nearly full multiplet of two-phonon MS states identified
 C. Fransen et al. PRC 67, 024307 (03)



Do we expect similar isovector excitations in nuclei close to doubly-magic nuclei...?

Mixed-symmetry states in 208Pb region?

MSS in vibrator-like nuclei

$A \approx 90$ $A \approx 130-140$
 $^{94,96}\text{Mo}$ ^{132}Te
 ^{92}Zr $^{128-134}\text{Xe}$
 ^{96}Ru ^{134}Ba
 $^{136-138}\text{Ce}, ^{140}\text{Ce}$
 $^{140}\text{Nd}(?), ^{144}\text{Nd}$

N. Pietralla, P. von
 Brentano, A.F.
 Lisetskiy, Prog. Part.
 Nucl. Phys. 60, 225
 (2008).

Z	206Po 8.8 D ε: 94.55% α: 5.45%	207Po 5.80 H ε: 99.98% α: 0.02%	208Po 2.898 Y α: 100.00% ε: 4.0E-3%	209Po 102 Y α: 99.52% ε: 0.48%	210Po 138.376 D α: 100.00%	211Po 0.516 S α: 100.00%	212Po 0.299 μS α: 100.00%	213Po 3.72 μS α: 100.00%	214Po 164.3 μS α: 100.00%
83	205Bi 15.31 D ε: 100.00%	206Bi 6.243 D ε: 100.00%	207Bi 31.55 Y ε: 100.00%	208Bi 3.68E+5 Y ε: 100.00%	209Bi STABLE 100%	210Bi 5.012 D β-: 100.00% α: 1.3E-4%	211Bi 2.14 M α: 99.72% β-: 0.28%	212Bi 60.55 M β-: 64.06% α: 35.94%	213Bi 45.59 M β-: 97.80% α: 2.20%
82	204Pb ≥1.4E+17 Y 1.4% α	205Pb 1.73E+7 Y ε: 100.00%	206Pb STABLE 24.1%	207Pb STABLE 22.1%	208Pb STABLE 52.4%	209Pb 3.253 H β-: 100.00%	210Pb 22.20 Y β-: 100.00% α: 1.9E-6%	211Pb 36.1 M β-: 100.00%	212Pb 10.64 H β-: 100.00%
81	203Tl STABLE 29.524%	204Tl 3.783 Y β-: 97.08% ε: 2.92%	205Tl STABLE 70.48%	206Tl 4.202 M β-: 100.00%	207Tl 4.77 M β-: 100.00%	208Tl 3.053 M β-: 100.00%	209Tl 2.161 M β-: 100.00%	210Tl 1.30 M β-: 100.00% β-n: 7.0E-3%	211Tl >300 NS β-
80	202Hg STABLE 29.86%	203Hg 46.594 D β-: 100.00%	204Hg STABLE 6.87%	205Hg 5.14 M β-: 100.00%	206Hg 8.32 M β-: 100.00%	207Hg 2.9 M β-: 100.00%	208Hg 41 M β-: 100.00%	209Hg 35 S β-: 100.00%	210Hg >300 NS β-
	122	123	124	125	126	127	128	129	N

^{212}Po

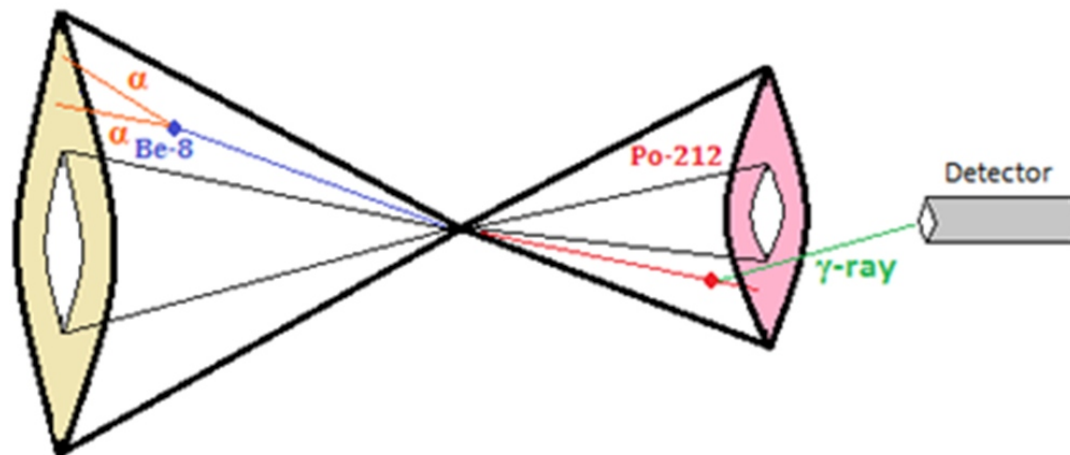
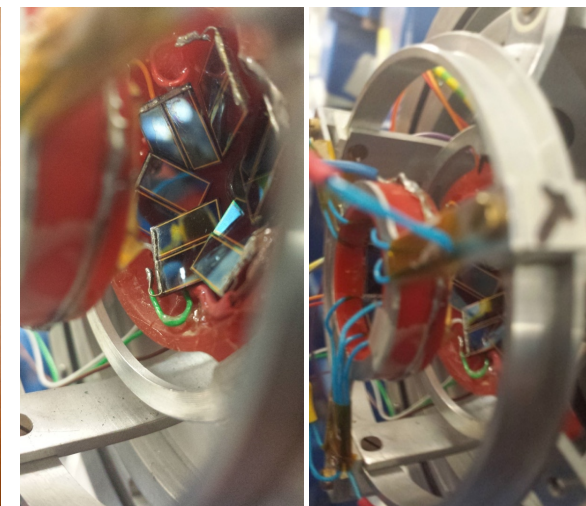
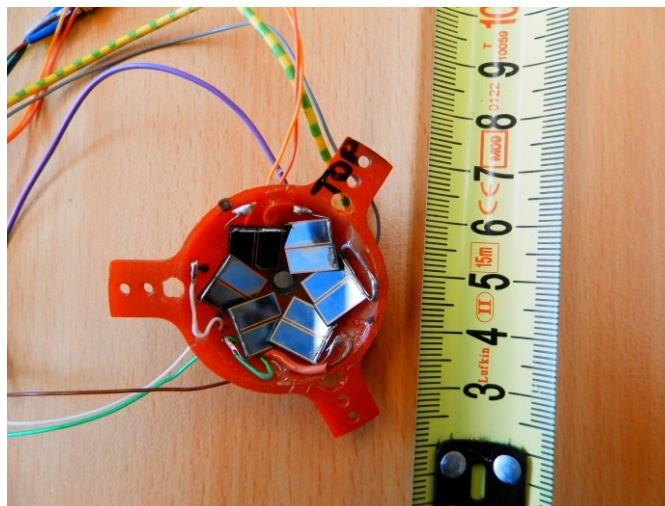
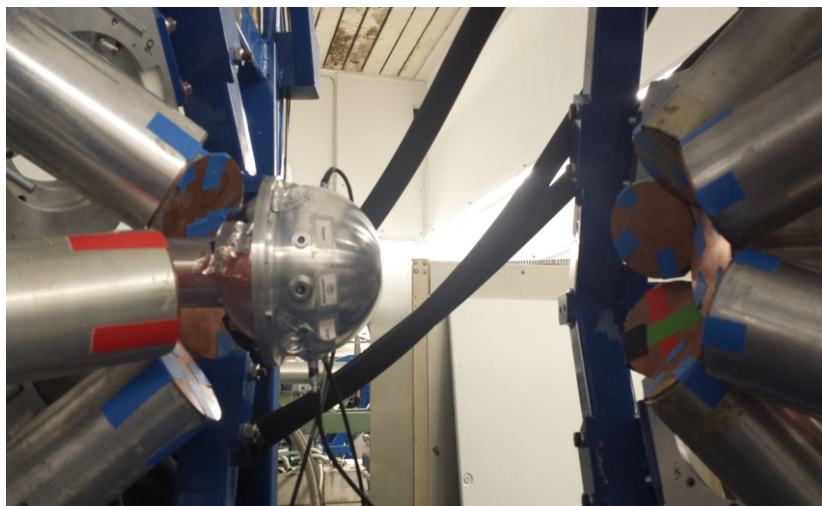
- Can we identify excited 2^+ states connected to the 2^+_{11} state with strong M1 transitions?
- Can we interpret these states as MSSs?

Experiment on ^{212}Po @ Cologne FN Tandem

G. Rainovski, D. Kocheva, K. Gladnishki, M. Djongolov,
Sofia University, Bulgaria



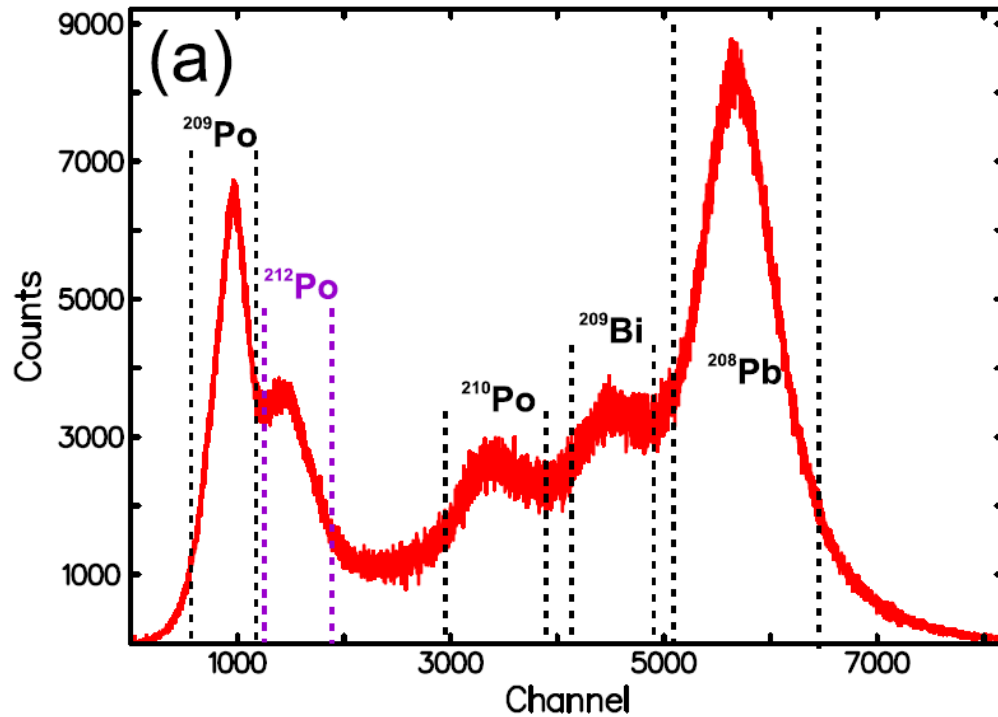
- Reaction $^{208}\text{Pb}(^{12}\text{C}, ^8\text{Be})^{212}\text{Po}$ @ 62 MeV ($V_{\text{col}} \approx 64$ MeV), target 10 mg/cm 2 ^{208}Pb
 - 5 HPGe detectors at 142.3° , 6 HpGe at 35.0° , and 1 HPGe at 0°
 - array of 6 solar cells (10 mm \times 10 mm), angular range $116.8^\circ - 167.2^\circ$: trigger $\gamma - \alpha$ or $\gamma - \gamma$



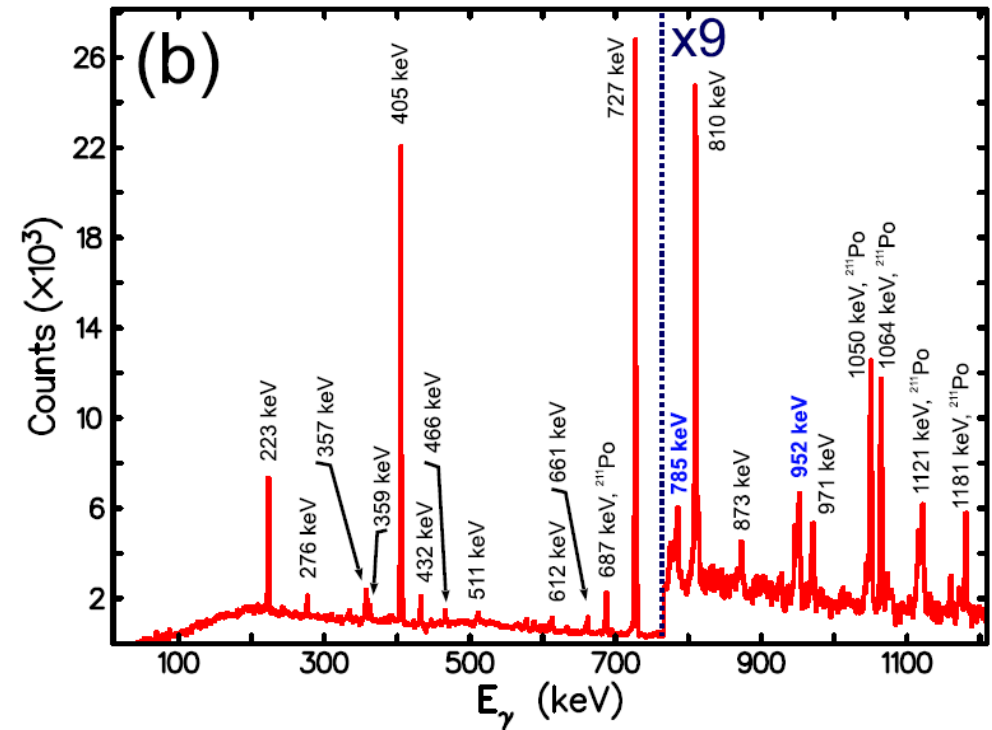
$$\langle v_0(^{212}\text{Po}) / c \rangle \approx 0.9\%$$

Experiment on ^{212}Po @ Cologne FN Tandem

G. Rainovski, D. Kocheva, K. Gladnishki, M. Djongolov,
Sofia University, Bulgaria



Solar cell spectrum



γ -ray spectrum of ^{212}Po
gated on $^8\text{Be} / 2\alpha$ channel

DSAM lineshape fits ^{212}Po

785.3 keV

$2^+_2 \rightarrow 2^+_1$

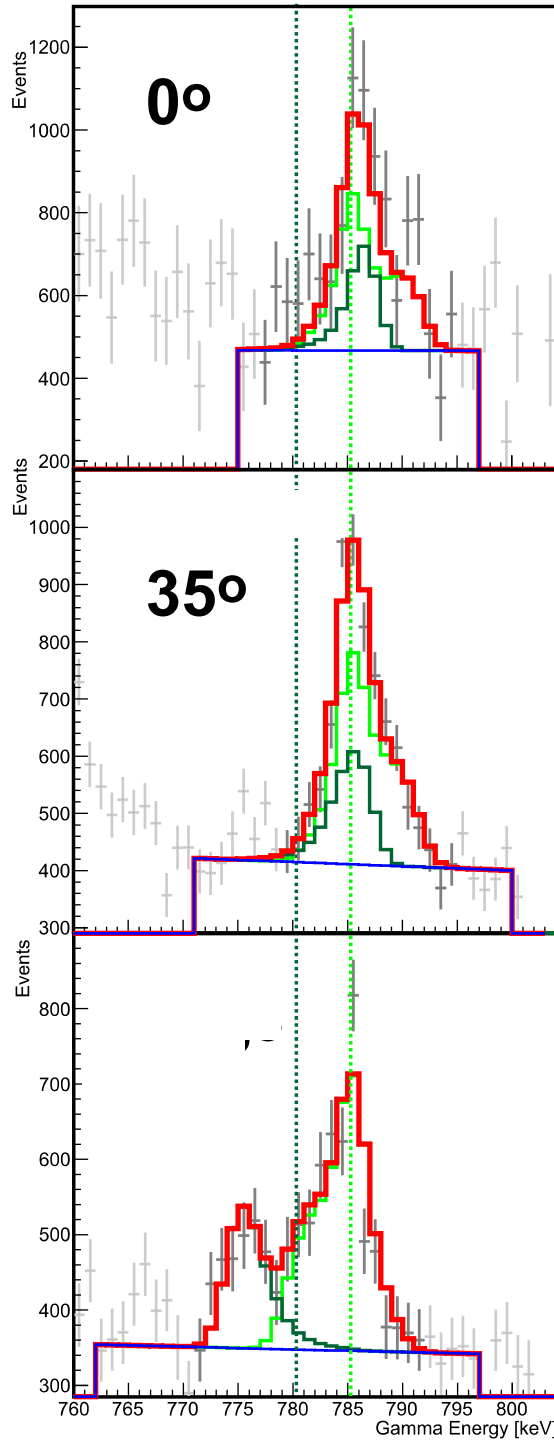
2^+_2 @ 1512 keV

Fast feeding only

$\tau = 0.75(5)$ ps

$\delta = +0.09(3)$

BR=100(1)/26(3)



952.1 keV

$2^+_3 \rightarrow 2^+_1$

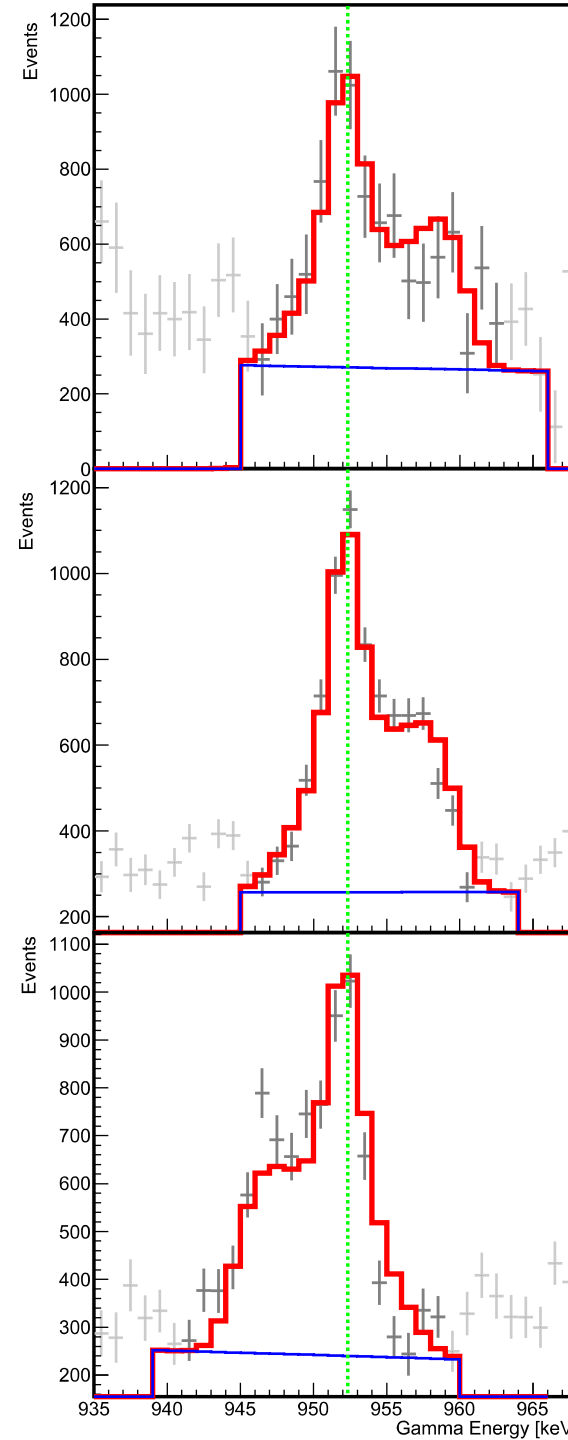
2^+_3 @ 1679 keV

Fast feeding only

$\tau = 0.80(3)$ ps

$\delta = +0.65(50)$

BR=100(19)/25(8)



D. Kocheva,
G. Rainowski

DSAM lineshape fits ^{212}Po

785.3 keV

$2^+_2 \rightarrow 2^+_1$

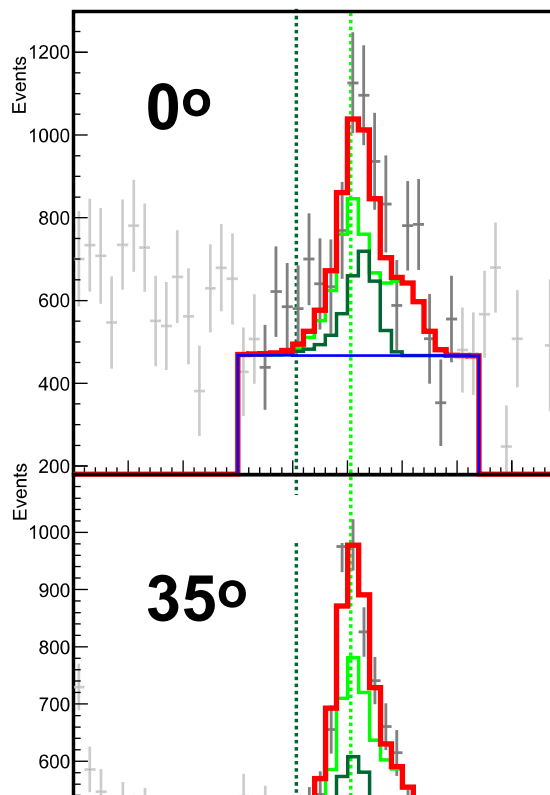
2^+_2 @ 1512 keV

Fast feeding only

$\tau = 0.75(5)$ ps

$\delta = +0.09(3)$

BR=100(1)/26(3)



952.1 keV

$2^+_3 \rightarrow 2^+_1$

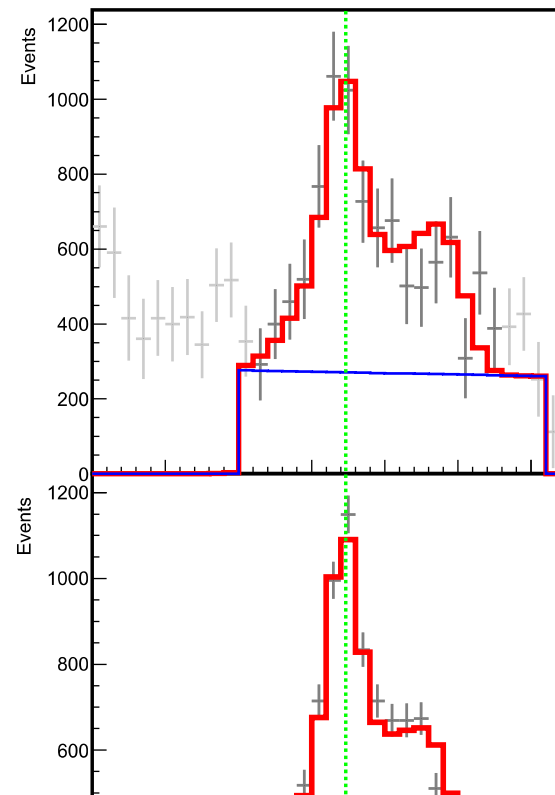
2^+_3 @ 1679 keV

Fast feeding only

$\tau = 0.80(3)$ ps

$\delta = +0.65(50)$

BR=100(19)/25(8)



	2^+_2 @ 1512 keV	2^+_3 @ 1679 keV
$B(M1; 2^+_i \rightarrow 2^+_1)$ (μ_N^2)	0.119(8)	$0.042^{+0.027}$
$B(E2; 2^+_i \rightarrow 2^+_1)$ ($e^2\text{fm}^4$)	22(2)	278(255)
$B(E2; 2^+_i \rightarrow 0^+_1)$ ($e^2\text{fm}^4$)	28(4)	20(5)

Shell model calculation for 2_1^+ , 2_2^+ in ^{212}Po

Single-shell approximation + empirical interaction from neighboring nuclei (P. Van Isacker)

$$^{212}\text{Po}: \quad ^{208}\text{Pb} + \nu(2g_{9/2})^2 + \pi(1h_{9/2})^2$$

$$\text{Basis states: } |(2g_{9/2})^2 J_\nu, (1h_{9/2})^2 J_\pi; J\rangle \equiv |J_\nu J_\pi J\rangle$$

$$\langle J_\nu J_\pi J | \hat{H} | J'_\nu J'_\pi J \rangle = (V_{\nu\nu}^{J_\nu} + V_{\pi\pi}^{J_\pi}) \delta_{J_\nu J'_\nu} \delta_{J_\pi J'_\pi} + 4\sqrt{(2J_\nu+1)(2J_\pi+1)(2J'_\nu+1)(2J'_\pi+1)} \sum_R \begin{bmatrix} j_\nu & j_\pi & J_\pi & J_\nu \\ R & j_\pi & J & j_\nu \\ j_\nu & j_\pi & J'_\pi & J'_\nu \end{bmatrix} V_{\nu\pi}^R$$

$V_{\nu\nu}^{J_\nu}$: from the experimental spectrum ($0^+ - 8^+$) of ^{210}Pb (2ν in $2g_{9/2}$)

$V_{\pi\pi}^{J_\pi}$: from the experimental spectrum ($0^+ - 8^+$) of ^{210}Po (2π in $1h_{9/2}$)

$V_{\nu\pi}^R$: from the experimental spectrum ($0^- - 9^-$) of ^{210}Bi

} seniority spectra

$$|2_1^+\rangle = 0.488 |J_\nu = 0, J_\pi = 2, J = 2\rangle + 0.819 |J_\nu = 2, J_\pi = 0, J = 2\rangle + \dots \quad \mathbf{87\%}$$

$$|2_2^+\rangle = 0.813 |J_\nu = 0, J_\pi = 2, J = 2\rangle - 0.517 |J_\nu = 2, J_\pi = 0, J = 2\rangle + \dots \quad \mathbf{93\%}$$

→ Consist of proton and neutron **S** ($J_{\nu(\pi)}=0$) and **D** ($J_{\nu(\pi)}=2$) pairs

2_2^+ state at 1512 keV isovector excitation of ^{212}Po , but:

Both the experimental results and the theoretical description show that these are not collective states!

Conclusion

- Transition strengths determined from level lifetimes allow to draw unique conclusions about nuclear structure.
- Overview about methods for lifetime determination used by our group:
 - Recoil Distance Doppler-shift method (Plunger)
 - Fast timing with delayed $\gamma\gamma$ -coincidences or $e^- - \gamma$ coincidences
 - Doppler-shift attenuation method
- Shape coexistence in neutron deficient Hg isotopes
- Hints for X(5) critical point symmetry in neutron deficient Os isotopes
- Observation of isovector excitations in ^{212}Po

Collaboration



Universität
zu Köln

A. Blazhev, T. Braunroth, A. Dewald, C. Fransen, R.-B. Gerst, A. Goldkuhle, A. Hennig, J. Jolie, J. Litzinger, C. Müller-Gattermann, J.-M. Regis, M. Rudigier, N. Saed-Samii, D. Wölk



JYVÄSKYLÄN YLIOPISTO
UNIVERSITY OF JYVÄSKYLÄ

T. Grahn, K. Auranen, P.T. Greenlees, A. Herzan, U. Jakobsson, R. Julin, S. Juutinen, J. Konki, M. Leino, P. Peura, P. Rahkila, P. Ruotsalainen, M. Sandzelius, J. Saren, C. Scholey, J. Sorri, S. Stolze, J. Uusitalo



D. Kocheva, G. Rainovski, K. Gladnishki, M. Djongolov



Sofia, Bulgaria

P. Petkov

G. de Angelis, L. Corradi, E. Fioretto, A. Goasduff, A. Gottardo, D.R. Napoli, A. Stefano, J.J. Valiente-Dobon

D. Bazzacco, S. Lenzi, S. Lunardi, R. Menegazzo, D. Mengoni, G. Montagnoli

R. Stegmann, N. Pietralla, C. Stahl, L. Cortes, Th. Möller, C. Bauer, M. Scheck, V. Werner, C. Schramm, M. Lettmann



TECHNISCHE
UNIVERSITÄT
DARMSTADT